

Copyright Warning & Restrictions

The copyright law of the United States (Title 17, United States Code) governs the making of photocopies or other reproductions of copyrighted material.

Under certain conditions specified in the law, libraries and archives are authorized to furnish a photocopy or other reproduction. One of these specified conditions is that the photocopy or reproduction is not to be “used for any purpose other than private study, scholarship, or research.” If a user makes a request for, or later uses, a photocopy or reproduction for purposes in excess of “fair use” that user may be liable for copyright infringement,

This institution reserves the right to refuse to accept a copying order if, in its judgment, fulfillment of the order would involve violation of copyright law.

Please Note: The author retains the copyright while the New Jersey Institute of Technology reserves the right to distribute this thesis or dissertation

Printing note: If you do not wish to print this page, then select “Pages from: first page # to: last page #” on the print dialog screen

The Van Houten library has removed some of the personal information and all signatures from the approval page and biographical sketches of theses and dissertations in order to protect the identity of NJIT graduates and faculty.

ABSTRACT

PHOTONIC CRYSTALS COMPOSED OF THICK INDUCTIVE AND CAPACITIVE MESHES

**by
Jay Shah**

The transmission properties of metal meshes are studied for single meshes, photonic double layers and photonic crystals. Simulations are performed with the Flomerics Micro-Stripes program for light of infrared and millimeter wavelengths. The Micro-Stripes program solves Maxwell's equations numerically and, for simulations of the transmittance of metal meshes, has been proven as good as an experiment. Input data are the geometrical parameters, the indices of refraction and the conductivity, chosen according to the Drude model. The light is assumed to be at normal incidence and the simulation results are compared with experiments.

Single layers of inductive meshes are studied for a range of metal thicknesses and opening sizes. Rectangular structures of cross, square and circular shaped openings and hexagonal structures with hexagonal openings are discussed for the same length of cross and square shapes and diameters of circles and hexagonal openings. The resulting spectra are interpreted with resonance modes of the surface waves, appearing at wavelength range larger than the periodicity constant, the wave guide modes and Wood anomaly at wavelength equal to the periodicity constant, and the diffraction region at shorter wavelength. A very desirable filter characteristic with 10% band width and 84% transmission was obtained for circular opening.

Photonic double layers are two meshes with lined-up openings at different separations. The layers are chosen to be thick inductive meshes and the transmission studied over a range of separations smaller than the resonance wavelength of the meshes. The results show that tunable filters may be constructed with a particular separation range.

Photonic crystals are studied, made of metal spheres supported by a dielectric medium with index close to one. A layered structure is assumed, with layers considered as thick capacitive meshes. The transmittance at normal incidence is studied for photonic crystals of Simple Cubic, Body-centered Cubic and Face-centered Cubic structures. The simulations are performed and interpreted with resonance mode of one layer and stacking mode of many layers. The agreement with experiments is excellent.

**PHOTONIC CRYSTALS COMPOSED OF THICK INDUCTIVE
AND CAPACITIVE MESHES**

**by
Jay Shah**

**A Thesis
Submitted to the Faculty of the
New Jersey Institute of Technology
In Partial Fulfillment of the Requirements for the Degree of
Master of Science in Electrical Engineering**

August 2003

APPROVAL PAGE

**PHOTONIC CRYSTALS COMPOSED OF THICK INDUCTIVE
AND CAPACITIVE MESHES**

Jay Shah

Dr. Karl D. Möller, Thesis Advisor
Research Professor, Department of Physics, NJIT

Aug 18/03
Date

Dr. Haim Grebel, Thesis Co-Advisor
Professor, Department of Electrical and Computer Engineering, NJIT

Aug 18, 03
Date

Dr. Marek Sosnowski, Committee Member
Professor, Department of Electrical and Computer Engineering, NJIT

August 18, 2003
Date

Blank Page

This thesis is dedicated to my parents and my brother whose constant love and support helped me throughout my education

BIOGRAPHICAL SKETCH

Author: Jay Shah

Degree: Master of Science

Date: August 2003

Date of Birth:

Place of Birth:

Undergraduate and Graduate Education:

- Master of Science in Electrical Engineering
New Jersey Institute of Technology, Newark, NJ, 2003
- Bachelor of Science in Electronics Engineering,
Vishwakarma Institute of Technology, Pune, India, 2000

Major: Electrical Engineering

ACKNOWLEDGMENT

I would like to recognize and thank my thesis advisor, Dr. Karl Dieter Möller, whose patience and guidance helped me, carry out the thesis work satisfactorily.

I convey my sincere thanks to Dr. Haim Grebel for his advice and support throughout my work and enlightening me through useful discussions.

I thank Dr. Marek Sosnowski for his participation and many useful suggestions in my work.

My sincere thanks to Dr. Oren Sternberg and Dr. John Tobias at Naval Research Laboratory and US Army Communications Electronics Command, respectively for providing experimental results for comparison.

My effort would not be possible without the funding support of the Electronic Imaging Center (NJIT).

Last, but certainly not least I would like to recognize my parents and my brother for their encouragement and understanding over the course of years of this work.

TABLE OF CONTENTS

Chapter	Page
1 INTRODUCTION	1
2 MODEL SIMULATIONS	6
2.1 Single Layer Thin and Thick Metal Meshes.....	6
2.2 Photonic Double Layer	7
2.3 Metallodielectric Photonic Crystals.....	8
2.4 Transmission Line Theory.....	8
2.4.1 Inductive Mesh as Oscillator	8
2.4.2 Capacitive Mesh as Oscillator	9
2.4.3 Cascading Matrices.....	9
2.4.4 Limitations of the Transmission Line Theory	10
2.5 Transmission Line Theory and Interaction of Oscillators	10
2.6 Micro-Stripes Simulation Program.....	11
2.6.1 Simulations and Experimental Results	11
2.6.2 The Input Data	12
2.6.3 The Output Data	13
2.6.4 Filtering Technique.....	14
2.6.5 Limitations of the Micro-Stripes Calculations.....	14
3 RESULTS	15
3.1 Single Layer Thick Metal Meshes.....	15
3.1.1 Geometrical Parameters	15
3.1.2 Modes of Meshes	16

TABLE OF CONTENTS
(Continued)

Chapter	Page
3.1.3 Rectangular Arrangement with Cross Shape Opening	16
3.1.3.1 Geometrical Parameters	16
3.1.3.2 Fixed Thickness and Varying Opening.....	17
3.1.3.3 Fixed Opening and Varying Thickness.....	18
3.1.4 Rectangular Arrangement with Square Shape Opening	19
3.1.4.1 Geometrical Parameters	19
3.1.4.2 Experimental Results	20
3.1.4.3 Fixed Thickness and Varying Opening.....	21
3.1.4.4 Fixed Opening and Varying Thickness.....	22
3.1.5 Rectangular Arrangement with Circular Shape Opening	23
3.1.5.1 Geometrical Parameters	23
3.1.5.2 Experimental Results	24
3.1.5.3 Fixed Thickness and Varying Opening.....	25
3.1.5.4 Fixed Opening and Varying Thickness.....	26
3.1.6 Hexagonal Arrangement of Circular Shape Opening	28
3.1.6.1 Geometrical Parameters	28
3.1.6.2 Experimental Results	29
3.1.6.3 Fixed Thickness and Varying Opening.....	30
3.1.6.4 Fixed Opening and Varying Thickness.....	31
3.1.7 Summary	32
3.2 Photonic Double Layer of Thick Cross Shaped Inductive Meshes	34

TABLE OF CONTENTS
(Continued)

Chapter	Page
3.2.1 Two 2 μ m Thick Meshes	35
3.2.2 Two 4 μ m Thick Meshes	36
3.2.3 Two 11 μ m Thick Meshes	37
3.2.4 Two 5.5 μ m Thick Meshes as Tunable Filters.....	38
3.2.4.1 Wave Guide Modes.....	38
3.2.4.2 Stacking Modes.....	39
3.2.5 Summary	40
3.3 Metallodielectric Photonic Crystal	41
3.3.1 Simple Cubic Photonic Crystals	42
3.3.1.1 Dependence on Number of Layers	43
3.3.1.2 Dependence on Sphere Diameter 'd'	46
3.3.1.3 Dependence on Separation 's' of Layers	47
3.3.1.4 Transmission Line Theory	49
3.3.2 BCC Photonic Crystals	50
3.3.2.1 Dependence on Number of Layers	50
3.3.2.2 Transition of BCC to Simple Cubic Photonic Crystal for a = 15mm.....	53
3.3.3 FCC Photonic Crystal	55
3.3.3.1 Experimental Result of Transmission through FCC PC.....	55
3.3.3.2 Simulations of Transmission through FCC PC.....	56
3.3.4 Summary	57

TABLE OF CONTENTS
(Continued)

Chapter	Page
4 DISCUSSIONS.....	58
4.1 Single Layer Thick Metal Meshes.....	58
4.2 Photonic Double Layer of Thick Cross Shaped Inductive Meshes	59
4.3 Metallodielectric Photonic Crystals.....	60
5 CONCLUSIONS.....	61
REFERENCES	62

LIST OF FIGURES

Figure	Page
1.1 Inductive Mesh (a), Capacitive Mesh (b), geometric parameters of the mesh (c)	1
1.2 Thick inductive (left) and capacitive (right) metal meshes	3
1.3 Schematic of photonic double layers and crystals.(a) Double layer. The openings of the meshes may be lined-up or shifted. (b) Crystal. The openings of the second and forth mesh may be lined-up with the first or third mesh or shifted.....	4
2.1 (a) Schematic of light incidence on a thin single layer. The light excites surface waves on both sides of the layer, and light with wavelengths around the resonance is transmitted, the other light reflected. (b) Schematic of light incidence on a thick single layer. In addition to the surface waves, waveguide modes are excited, appearing with wavelength close to the periodicity constant.....	6
3.1 Rectangular arrangement of cross openings. Black is Metal and White is opening in (a). 3-D view of (a) is (b). The parameters are periodicity constant g , separation $2a$, arm width $2b$, cross width d and thickness t	17
3.2 Cross shaped opening in a rectangular mesh with fixed thickness of $0.43g$ and varying openings.....	18
3.3 Cross shaped opening in a rectangular mesh with fixed opening of $0.68g$ and varying thickness	19
3.4 Rectangular arrangement of square openings. Black is metal and White is opening in (a). The parameters are periodicity constant g , length of square opening d and separation $2a$. (b) is 3-D view of (a). thickness t	20
3.5 Experimental transmittance of Square meshes with 1000, 1500 and 2000 lines/inch	21
3.6 Square shaped opening in a rectangular mesh with fixed thickness of $0.43g$ and varying opening	22
3.7 Square shaped opening in a rectangular mesh with fixed opening of $0.68g$ and varying thickness	23

LIST OF FIGURES
(Continued)

Figure	Page
3.8 Rectangular arrangement of circular openings. Black is metal and White is opening in (a). The parameters are periodicity constant g , circle diameter d and separation $2a$. (b) is 3-D view of (a). thickness t	24
3.9 Transmission spectra of a circular mesh investigated experimentally ²⁸ in the nm region. The inset shows the cross section of the film, White is Ag film, White and black is Ni film coated with Ag and Black is Ni film	25
3.10 Circular shaped opening in a rectangular mesh with fixed thickness of $0.43g$ and varying opening	26
3.11 Circular shaped opening in a rectangular mesh with fixed opening of $0.68g$ and varying thickness	27
3.12 Circular shaped opening with 84% transmittance and a bandwidth of 10%	28
3.13 Hexagonal arrangement of circular openings. Black is metal and White is opening in (a). The parameters are periodicity constant g , circle diameter d (b) is 3-D view of (a). thickness t	29
3.14 Experimental hexagonal shaped mesh with various opening ⁵ . The resonance and wave guide mode are clearly seen	30
3.15 Hexagonal arrangement of holes with fixed thickness of $0.43g$ and varying opening	31
3.16 Hexagonal arrangement of holes with fixed opening of $0.68g$ and varying thickness.	32
3.17 A specific case of 3 shapes, hexagonal, circular and square type mesh. The specifications for the 3 meshes are $d_n = 0.58$ and $t_n = 0.43$	33
3.18 Two cross-shaped Inductive aligned meshes.....	34
3.19 Schematic of two aligned meshes at various separations	35
3.20 Transmittance of two thin metal meshes of thickness $2\mu\text{m}$ at separations 1, 3, 4, 7, 9 and $11\mu\text{m}$	35

**LIST OF FIGURES
(Continued)**

Figure	Page
3.21 Transmittance of two thin metal meshes of thickness $4\mu\text{m}$ at separations 1, 4, 5, 6, 9 and $12\mu\text{m}$	36
3.22 Transmittance of cross shaped meshes of thickness $11\mu\text{m}$ at separations of $4\mu\text{m}$ and $8\mu\text{m}$. The peak at around $36\mu\text{m}$ is the resonance wavelength of the meshes.....	37
3.23 Transmittance of two meshes of thickness $5.5\mu\text{m}$ at separations of 0.4, 1, 2, 3, 4 and $5\mu\text{m}$	38
3.24 Expanded plot of section for separation of 0.4, 1, 2, 3, 4 and $5\mu\text{m}$	39
3.25 Transmittance of two meshes of thickness $5.5\mu\text{m}$ and separation of 11, 12, 13, 14, 15, $16\mu\text{m}$	40
3.26 Two layers of Cubic Photonic Crystal (a); Three layers of Body Centered Cubic (BCC) (b); Three layers of Face Centered Cubic (FCC) (c)	42
3.27 Micro-Stripes calculated transmission of a Cubic crystal with 1 to 10 stacked layers. The parameters of the crystal are $a = 15\text{mm}$, $d = 6.35\text{mm}$ and $s = 15\text{mm}$	43
3.28 Micro-Stripes calculated transmission of a Cubic crystal with 1 to 10 stacked layers. The parameters of the crystal are $a = 15\text{ mm}$, $d = 6.35\text{ mm}$ and $s = 15\text{ mm}$	44
3.29 Experimental transmission of Simple Cubic crystal with crystal lattice $a = 20\text{ mm}$. The parameters of the crystal are $d = 6.35\text{ mm}$ and $s = 20\text{ mm}$	45
3.30 Micro-Stripes calculated Cubic crystal with crystal lattice $a = 20\text{ mm}$. The other parameters are $d = 6.35\text{ mm}$ and $s = 20\text{ mm}$	46
3.31 Transmission of Simple Cubic crystal depending on the sphere diameter $d = 4, 6.35, 7$ and 8 mm , $a = 15\text{ mm}$	47
3.32 Transmission of Cubic crystal with Separation between the Stacking Layers 's' varied as 7.5, 15, and 20 mm . The other crystal parameters are $a = 15\text{ mm}$ and $d = 6.35\text{ mm}$	48

**LIST OF FIGURES
(Continued)**

Figure	Page
3.33 Resonance and stacking mode peaks for Simple Cubic crystal calculated with Transmission Line Theory.....	49
3.34 Micro-Stripes calculated transmission of a BCC crystal with 1 to 10 stacked layers. The parameters of the crystal are $a = 15 \text{ mm}$, $d = 6.35$, $d_b = 6.35 \text{ mm}$ and $s = 7.5 \text{ mm}$	51
3.35 Experimentally measured transmission of BCC Crystal with $a = 20 \text{ mm}$. The crystal parameters are $d = 6.35 \text{ mm}$, $d_b = 6.35 \text{ mm}$ and $s = 10 \text{ mm}$	52
3.36 Micro-Stripes calculated transmission of a BCC crystal with 1 to 6 stacked layers. The parameters of the crystal are $a = 20 \text{ mm}$, $d = 6.35$, $d_b = 6.35 \text{ mm}$ and $s = 10 \text{ mm}$	53
3.37 Transition from Simple Cubic to BCC by increasing center diameter 'db' in steps of 0, 4, 5 and 6.35mm	54
3.38 Experimental result for FCC PC by Serpenguzel with $a = 15\text{mm}$ and $d = 6.35\text{mm}$	55
3.39 Micro-Stripes calculated transmission of an FCC crystal with 1 to 10 stacked layers. The crystal parameters are $a = 15\text{mm}$ and $d = 6.35\text{mm}$	56

CHAPTER 1
INTRODUCTION

Metal meshes have been used as filters and reflectors in the microwave and infrared wavelength region. In the microwave region, Culshaw¹ constructed cavities with high Q-value by using perforated metal plates as reflectors. Commercially available electroformed metal meshes have been used in far infrared by Ulrich et al.² as Fabry-Perot reflectors. These square shaped metal meshes, called by Ulrich³ inductive mesh showed low losses in the peak transmittance region. The inverse structure, first published by Ressler and Möller⁴, was called capacitive mesh.

Ulrich⁵ used a combination of inductive and capacitive meshes to manufacture cross shaped meshes, see Figure 1.1, and Chase and Joseph⁶ studied inductive cross shaped meshes in details. The inductive cross shaped metal meshes may be designed to have a more narrow band pass characteristic than square shaped inductive meshes and are of interest to the astrophysical community as band pass filters.

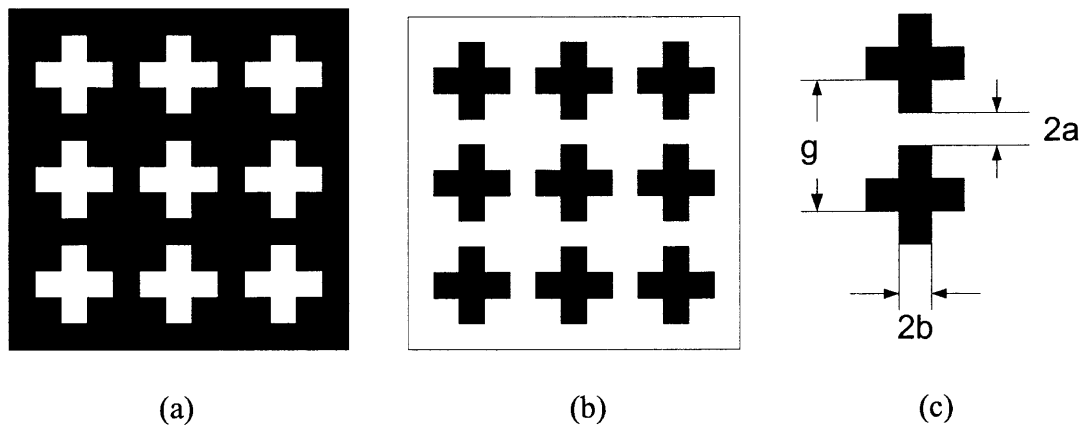


Figure 1.1 Inductive Mesh (a), Capacitive Mesh (b), geometrical parameters of the mesh (c).

Geometrical parameters of the mesh are the separation $2a$, width $2b$ and periodicity constant 'g' as shown in the figure above. In case of 3-Dimensional structures, another parameter thickness 't' of the mesh comes in picture.

An inductive metal mesh diffracts all light of wavelength shorter than the periodicity constant and reflects most of the light of wavelength larger than the periodicity constant. Inductive and capacitive meshes, according to Babinet's Principle, that is that complementary screens have complementary transmittance, have the same resonance wavelength, the inductive mesh in transmission, the capacitive in reflection. Proof of this principle will be seen in Chapter 2.

Thin inductive mesh structures are used in the millimeter and centimeter wave region "frequency sensitive surfaces" and used for antennas. Various structures of this type have been studied⁷.

Ulrich³ developed transmission line theory for monitoring multiple mesh filters and introduced the damped oscillator model. He used electromagnetic circuit elements for the description of a resonant wavelength of one mesh and studied arrays of metal meshes. Whitbourn and Compton⁸ improved the theory for applications to capacitive meshes with dielectric substrates. The theory is semi-empirical with parameters of the oscillator as input data. Inductive free standing cross shaped metal meshes have been produced by M. Rebbert et al.⁹, Porterfield et al.¹⁰, and Möller et al.¹¹.

Thick inductive and capacitive meshes, see Figure 1.2 show, in addition to the resonance mode of the thin mesh, for thicknesses larger than half the periodicity constant, a waveguide mode depending on the thickness of the mesh.

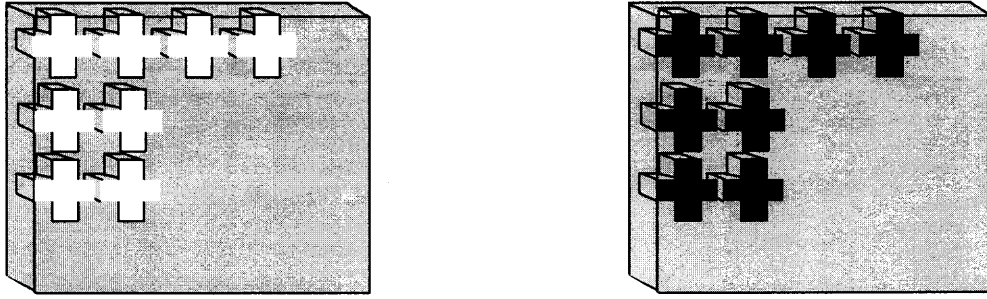


Figure 1.2 Thick inductive (left) and capacitive (right) metal meshes.

The incident light excites the waveguide mode by k-vector matching at wavelength close to the periodicity constant. This is a result of the periodicity condition for the electrical field, and the wavelength does not depend much on the shape and size of the openings. The waveguide mode transforms the spectrum of a capacitive mesh into one, similar to an inductive mesh. Resonance wavelength of the surface waves depends on the periodicity constant and the geometrical parameters.

Two metal mesh layers at a certain distance are recognized as photonic double layer if the openings of one mesh are lined up with the openings of the other, or shifted by $\frac{1}{2}$ of the periodicity constant in both rectangular direction, see Figure 1.3(a). Photonic crystals are shown in Figure 1.3(b). The openings of the second and forth mesh may be lined-up with the first or third mesh or shifted.

Metallodielectric photonic crystals, made of stacks of inductive meshes, have been studied experimentally^{13,14} and with simulations¹⁵. Serpengüzel¹⁶ has investigated metallodielectric crystals of the face centered cubic structure (Fcc) in the millimeter wave region. These crystals are made of metal spheres supported by dielectric material of refractive index around 1, and may be considered as stacks of capacitive meshes.

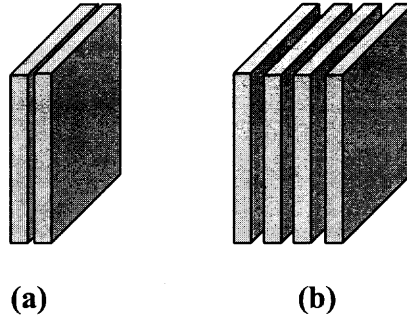


Figure 1.3 Schematic of photonic double layers and crystals.(a) Double layer. The openings of the meshes may be lined-up or shifted. (b) Crystal. The openings of the second and fourth mesh may be lined-up with the first or third mesh or shifted.

Similar crystals with simple cubic and body-centered cubic structures have been investigated in the millimeter region by Tobias¹⁷. The crystals were made of metal spheres, and the transmittance of structures for 1 to 6 layers measured.

Li et al.¹⁸ have studied theoretically the layered structures of dielectric and metallodielectric photonic crystals and found that layers with negative dielectric constant are described by dispersive elements, resulting in resonances of a single layer. The interpretation of the transmittance of multi-layer structures may therefore be done, by considering the resonance mode of one layer and the stacking mode of many layers. The stacking mode depends on the separation of the layers and corresponds to Bragg reflection.

In this thesis, Flomerics Micro-Stripes program¹⁹ is used for the simulations of the reflection of photonic double layers made of two inductive meshes and metallodielectric photonic crystals, of stacks of capacitive meshes. This program solves Maxwell's equations and uses as input data the geometrical parameters of the crystal, the refractive index of the dielectrics and the surface impedance of the metal. The Fourier modal method^{20,21} as well as other computational programs have shown that the Drude model of

conductivity is valid for the spectral region from the long wavelength, sub millimeter and millimeter region, to the short wavelength infrared.

The Micro-Stripes program may only be used for the aligned or shifted configuration of photonic double layers, photonic crystals, and the near field around the mesh surface, in the channels for thick meshes or in the gap between two meshes may be investigated. In contrast, transmission line theory does not include any alignment of the openings and results in the far field transmission of the mesh or mesh assembly. The usefulness of these types of multi-layer metal meshes as filters will be discussed.

CHAPTER 2

MODEL SIMULATIONS

2.1 Single Layer Thin and Thick Metal Meshes.

Thin metal meshes have a thickness small compared to the periodicity constant, about a few percent, while thick meshes have thickness comparable to the periodicity constant. The light is considered at normal incidence (z - direction) and induces two pairs of standing surface waves, one on the front and the other on the back side of the mesh²². The pair of standing waves consists of two surface waves propagating in opposite direction on the surface of the mesh (x, y direction) and is tightly coupled to the other pair through the openings, see Figure 1a. The resulting k vector is zero, because the incident wave has no component of the k vector in the x, y direction. The pairs of standing surface transforms the incident light into reflected and transmitted light.

The surface waves form a mode with the resonance depending on the size and shape of the openings. These modes have been studied extensively in antenna theory⁷.

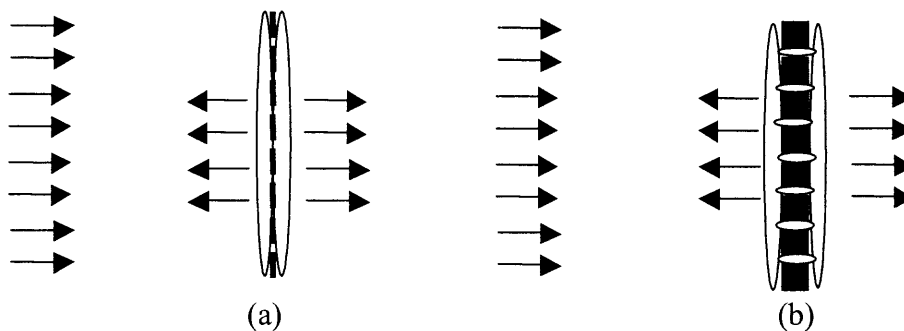


Figure 2.1 (a) Schematic of light incidence on a thin single layer. The light excites surface waves on both sides of the layer, and light with wavelengths around the resonance is transmitted, the other light reflected. (b) Schematic of light incidence on a thick single layer. In addition to the surface waves, waveguide modes are excited, appearing with wavelength close to the periodicity constant.

The incident light excites, by k vector coupling, a wave guide mode in the channel of the opening of a thick mesh. The wave guide mode has a wavelength close to the periodicity constant. Interaction of resonance and wave guide mode may shift the peak appearance to longer wavelength.

2.2 Photonic Double Layer

Two metal mesh layers at a certain distance are recognized as photonic double layer if the openings of one mesh are lineup with the openings of the other, or shifted by $\frac{1}{2}$ of the periodicity constant in both rectangular direction¹⁵. The plane wave is incident in the z direction perpendicular to these meshes. Thick cross shaped metal meshes show resonance and wave guide mode. The resonance mode depends on the geometrical shape and size of the openings⁶, but not much on the thickness of the mesh, while the wave guide modes depend little on the shape and size of the openings, but much on the thickness of the mesh. In addition to the resonance and wave guide mode, the separation of the two meshes will show a third type of mode, the stacking modes, depending on the separation of the meshes. These modes are different from “Fabry Perot” modes²¹, as observed when using two non periodic reflecting plates. The meshes may be considered as oscillators and the stacking mode, at distances depending on the wavelength of the resonance modes, is generated by the interaction of the meshes¹⁵.

2.3 Metallodielectric Photonic Crystals

Metal spheres are placed in stacks forming a layered structure^{16,17}. The layers are separated by a dielectric medium with dielectric constant close to air. These parameters along with the number of layers are varied for sphere arrangements, and reflection peaks are recorded for normal incidence light. . The reflection peaks are interpreted with two types of modes, the resonance mode of a single layer, corresponding to the resonance minimum of a capacitive mesh, and the resonance of the stacking modes, generated by the stack of equally spaced layers, corresponding to Bragg reflection.

2.4 Transmission Line Theory.

Ulrich developed transmission line theory for the calculation of reflectance and transmittance of thin metal meshes^{3,5}. The theory uses geometrical and electrical parameters for the description of optical properties, a short description is given²³. Ulrich's formulation has been corrected by Whitbourn and Compton⁸ and will be used here.

2.4.1 Inductive Mesh as Oscillator.

We consider an inductive thin metal mesh and describe the resonance oscillation by shunt impedance,

$$Y(\lambda) = 1/[a_1 - i(\omega_0 A_1)/\Omega(\lambda)], \quad (1)$$

where

$$\Omega(\lambda) = (g/\lambda\omega_0) - (\lambda\omega_0/g). \quad (2)$$

The periodicity constant of the mesh is g , the resonance frequency ω_0 , the bandwidth parameter $A1$ and the loss parameter $a1$. The input parameters ω_0 , $A1$, and $a1$ may be obtained from observations, simulations such as the Micro-Strips program or empirical formulas as shown hereafter.

2.4.2 Capacitive Mesh as Oscillator

When a capacitive mesh is considered, the impedance shunt impedance is

$$Y(\lambda) = 1/[a1 + i\Omega(\lambda)/(4\omega_0 A1)],$$

2.4.3 Cascading Matrices

It is convenient to use the cascading matrix formulation²⁴. Each element of the transmission line is presented by a 2 by 2 matrix. The waves on the left side of the impedance Y , are related by a matrix M to the waves on the right side as

$$\begin{aligned} b_1 &= m_{11} a_2 + m_{12} b_2 \\ a_1 &= m_{21} a_2 + m_{22} b_2 \end{aligned} \quad (3)$$

For $a_2 = 0$, that is no backwards traveling wave on the right side, one has for the ratio of the reflected wave b_1 to incident wave a_1

$$b_1/a_1 = -m_{12}/m_{22} \quad (4)$$

and for the ratio of the transmitted wave b_2 to the incident wave a_1

$$b_2/a_1 = 1/m_{22}. \quad (5)$$

The transmitted intensity is calculated from the (2,2) element of the resulting matrix presenting all elements in the transmission line.

2.4.4 Limitations of the Transmission Line Theory

To apply the transmission line theory to the calculation of one or more meshes, one needs as input data the resonance wavelength of the mesh, the separation and the refractive index of the media inside and out. Transmission line theory also ignores the periodicity of the mesh and the alignment of the geometrical features.

2.5 Transmission Line Theory and Interaction of Oscillators.

Transmission line theory can be used to study the transmission of two oscillators separated by the distance d in the transmission line. The result is the appearance of a new mode, called “stacking mode”. The stacking mode is not a Fabry-Perot mode, because the reflecting plates have a reflectivity of almost zero at resonance of the two layer structure. While the stacking mode depends on the resonance mode of the mesh and the separation, a Fabry-Perot mode depends on the reflectivity of the plates and the separation²⁵.

The study of interaction of two oscillators can be applied to the study of interaction of the resonance mode of each of two single meshes. The stacking mode is close to a Fabry Perot mode for wavelength much longer and also much smaller than the resonance wavelength of a single mesh. However, when the wavelength of the stacking mode approaches the resonance wavelength of a single mesh, the modes do not overlap, the non crossing rule applies. The term interaction is used here as done in perturbation theory. The original modes are used for the calculation and discussion and their wavelength is modified by the interaction terms, resulting e.g. for a change in a geometrical parameter.

The study of interaction of two oscillators can be applied to the study of the interaction of resonance and wave guide mode of a single mesh. The stacking mode is associated with the wave guide mode of thick cross shaped meshes, because of its dependence on the thickness²¹.

2.6. Micro-Stripes Simulation Program

2.6.1. Simulations and Experimental Results

The Micro-Stripes simulation program¹⁹ was employed for the simulations of layered periodic structures. The 2D periodic structures were generated by considering a unit cell with reflecting walls. The geometrical dimensions of shape and size of the particular structure under consideration are used as input parameters as well as the dielectric constant or conductivity of the material.

The transmittance of very accurately manufactured samples, produced by LIGA, were reproduced with the Micro-Stripes program. Cross shaped meshes with steep walls and flat surfaces of several thicknesses, made of Copper and Nickel, could be used for testing the program. The peak transmission wavelengths of resonance and wave guide modes agreed with experimental values with an average accuracy of 1%. The assumed bulk conductivity was corrected by intensity matching of the peaks and used from there on, for similar simulations. The Micro-Stripes program can be considered as good as experiment for simulations of single meshes, double layers and metallodielectric crystals, as presented in this thesis.

2.6.2 The Input Data

Micro-Stripes program provides an option of building the structure using its in-built features or importing the structure from other design programs for example CAD. In this thesis, all the structures were built using the in-built library of Microstripes, consisting of various structures and shapes. The program also provides a function of drilling through the built structure.

For Single Layer Thick Metal Meshes, the meshes were built inputting the length of the opening in case of cross and square opening and diameter in case of circles. The periodicity constant and the thickness of the mesh were the other input parameters. After a rectangular mesh was built, cross, square or circular openings were drilled through the mesh as required, with parameters length of the openings or the diameter.

In case of Photonic Double Layers, rectangular mesh with cross shaped openings was built using the periodicity constant, length of the arm and separation between the crosses. A similar mesh was duplicated at certain distance making it a double layer. These layers were aligned, and the separation between them was varied.

Layers of spheres were built in Metallodielectric Photonic Crystals. The spheres were built with the parameter 'd' as the diameter of the spheres, and adjacent spheres separated by crystal lattice constant. For body centered cubic crystal, a sphere at the center of the cubic crystal was an addition to the simple cubic crystal, and for face centered crystal each side of the cube has a center sphere.

A frequency range needs to be mentioned for each structure so that the transmission output can be observed only in that particular range. After the structures

were built as mentioned above, transmission of light through these structures was observed in the far field, using an incident plane wave in the z-direction.

2.6.3 The Output Data

After the simulation, the output file is plotted with transmittance vs. frequency in db scale. This file is exported to a text file. The text file is imported in an Excel sheet. Frequency is converted into wavelength by dividing speed of light by frequency. Transmittance is converted from db scale to percentage scale to give the percent transmission intensity. After the conversions mentioned above, the resultant data are filtered and then plotted.

2.6.4. Filtering Technique

Filtering of the output data from the Micro-Stripes program is required, in order to have a noise free curve, as much as possible. Introduction of noise in the simulated result is due to the fact that the structures are simulated at a high frequency. A unique method of filtering is used here.

The text file from Micro-Stripes is imported into the Excel sheet. After the conversion of frequency into wavelength and transmittance of percentage from db, the resultant figure is plotted in the excel sheet. It appears on the figure, that the same wavelength has various transmittance intensities. A filtering technique developed, was applied to this excel file.

Starting with the shortest wavelength, transmittance intensity comparable to the intensity of the previous wavelength would be selected from various transmittance values

in the excel file and a new file will be generated having one intensity value for each wavelength and in this matter the new noise free figure was plotted.

In this manner using the new technique the final result is obtained.

2.6.5. Limitations of the Micro-Stripes Calculations

The Micro-Stripes program gives quantitative accurate results in the wavelength region larger than the periodicity constant. Considering calculations for wavelength smaller than the periodicity constant makes the results only qualitative.

CHAPTER 3

RESULTS

3.1 Single Layer Thick Metal Meshes

Thick metal meshes of rectangular arrangement of cross, square and circular shape openings and hexagonal arrangement of holes are discussed. To describe the interaction process, a plane wave is assumed propagating in z direction, perpendicular to the surface of the mesh in the x - y plane. The incident light excites a pair of standing surface waves on the front and backside of the mesh. Most of the light is reflected and the transmitted light has maximum intensity at the resonance wavelength of the mesh. Along with the surface wave resonance, wave guide modes are excited, depending on the thickness of the mesh. The wave guide mode appears only for thick meshes, with a wavelength close to the periodicity constant. Cross shape meshes show an interaction of the resonance mode and the wave guide mode causing the resonance mode to shift to longer wavelength.

3.1.1 Geometrical Parameters

The common parameters that are applicable to all structures are described in this section. Additional parameters will be given in the respective sections of different arrangements. 'g' is the periodicity constant and has been chosen for the simulations to be $164 \mu\text{m}$. 'd' is the width of the cross or square in case of cross and square shape opening, respectively. In the case of circular and hexagonal opening, 'd' is the diameter of the holes, and 't' the thickness. In order to make the graphs more useful, the transmissions have been plotted as a function of the wavelength divided by periodicity constant 'g', called the normalized

wavelength. 'd' are divided by the periodicity constant 'g' and designated as 'dn'. Similarly thickness 't' divided by 'g' and designated as 'tn'. The arrangements with different openings have been simulated for fixed thicknesses $t = 0.43g$ and opening diameters $d = 0.58g, 0.64g, 0.68g$ and $0.78g$, as well for fixed diameters $d = 0.68g$ and thicknesses $t = 0.12g, 0.24g, 0.43g$ and $0.61g$.

3.1.2 Modes of Meshes

As mentioned in section 2.1, at normal incidence in z direction, wave guide mode along with surface wave resonance is observed. The interaction of resonance and wave guide modes of rectangular and hexagonal meshes has been studied. These meshes were examined in three segments: $\lambda < g$ the diffraction region, $\lambda = g$ the Wood anomaly where the wave guide modes start to appear, and at $\lambda > g$ where the surface wave resonance peak wavelength appears. In general, the transmission range increases with larger openings. The excited surface wave transfers the incident light into the reflected and transmitted light.

3.1.3 Rectangular Arrangement with Cross Shape Opening

3.1.3.1 Geometrical Parameters The structure with rectangular arrangement of cross shape opening is shown in Figure 3.1. Figure 3.1(a) shows the x-y view of the single layer metal structure. Black is metal and white are the cross openings. In addition to the parameters mentioned in section 3.1.1, '2a' is the separation of the crosses such that $2a = (g - d)$ and '2b' is the arm width of the cross such that $2b = d/3$. Figure 3.1 (b) is the three dimensional view of the structure.

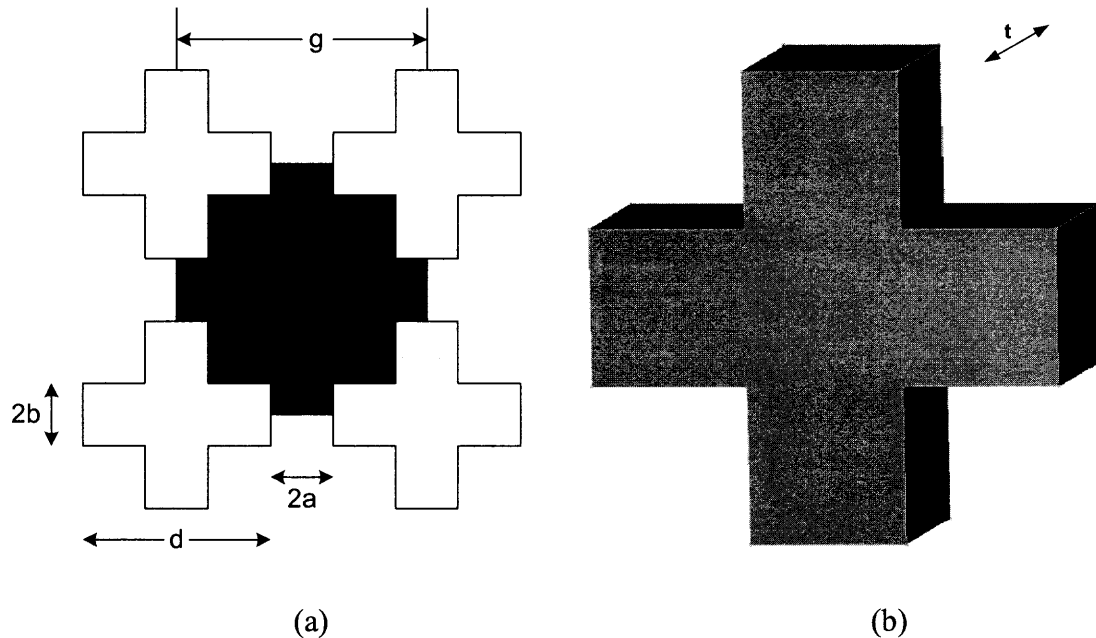


Figure 3.1 Rectangular arrangement of cross openings. Black is Metal and White is opening in (a). 3-D view of (a) is (b). The parameters are periodicity constant g , separation $2a$, arm width $2b$, cross width d and thickness t .

3.1.3.2 Fixed Thickness and Varying Opening

The simulated transmittance of resonance and wave guide modes of thick meshes with cross shape openings is shown in Figure 3.2. The wave guide mode appears at a normalized wavelength close to g and the resonance mode at higher wavelengths. With increase in openings the resonance mode shifts to a higher wavelength while the wave guide mode continues to remain at the same wavelength. The bandwidth of the resonance peak is in the 20% to 40% range increasing with the opening and transmittance to 80%. The diffraction region shows small transmission which is advantageous for use of Band pass filter.

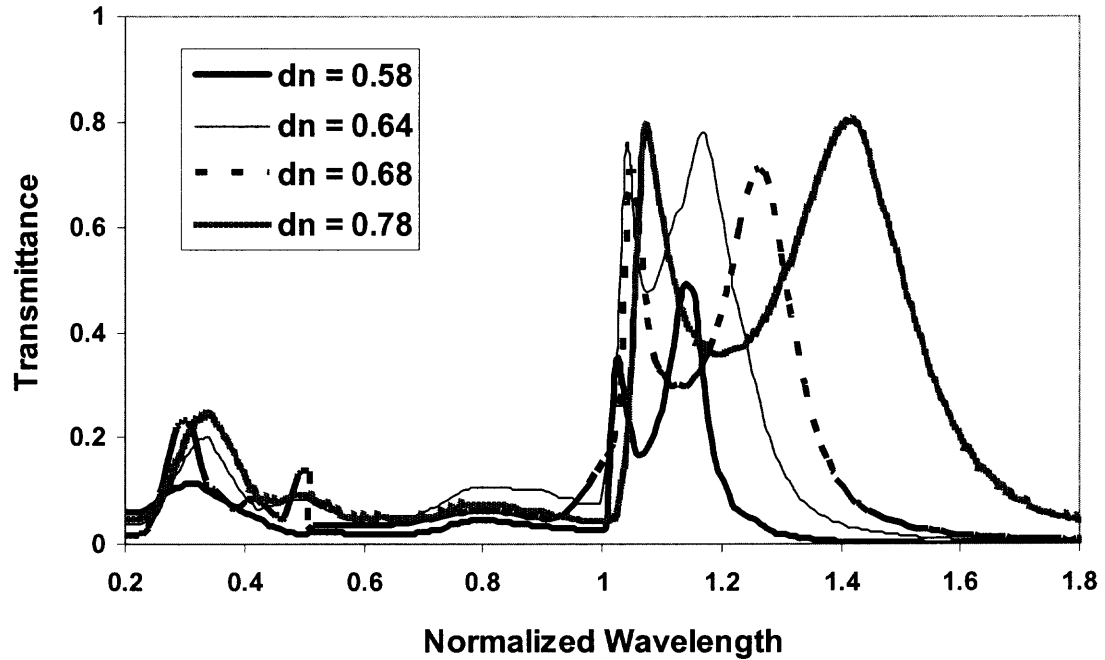


Figure 3.2 Cross shaped opening in a rectangular mesh with fixed thickness of $0.43g$ and varying openings.

3.1.3.3 Fixed Opening and Varying Thickness

The wave guide mode is not observed for thin meshes as shown in Figure 3.3 for $t_n = 0.12g$. As the thickness increases the wave guide mode begins to appear. At $t_n = 0.24g$, the wave guide mode appears with a normalized wavelength close to 1. As observed, with increased thickness, the wave guide mode shifts to a longer wavelength which shows more interaction with the resonance mode. As a result of this interaction the intensity of the resonance mode decreases and that of the wave guide mode increases with increase in thickness of the mesh with cross shape opening. The bandwidth remains the same in the 30% range and is not affected by change in the thickness of the mesh.

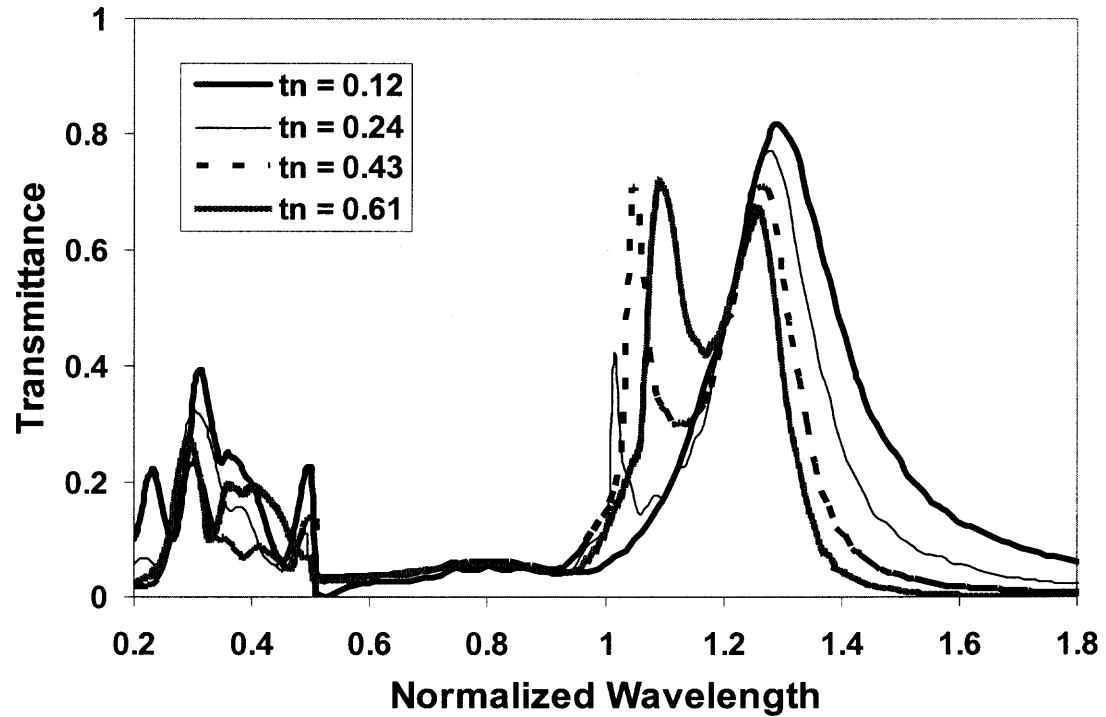


Figure 3.3 Cross shaped opening in a rectangular mesh with fixed opening of $0.68g$ and varying thickness.

3.1.4 Rectangular Arrangement with Square Shape Opening

3.1.4.1 Geometrical Parameters

Figure 3.4 shows rectangular arrangement of square shape openings. 'g' is the periodicity constant, 'd' is the side of each square and '2a' is the separation of the squares such that $2a = (g - d)$.

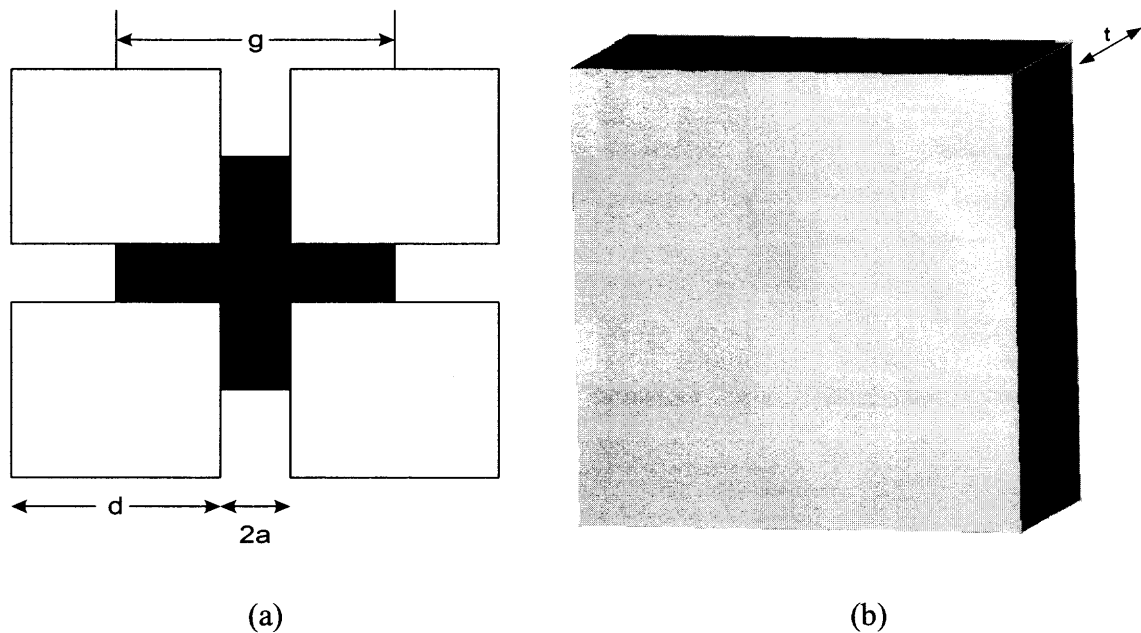


Figure 3.4 Rectangular arrangement of square openings. Black is metal and White is opening in (a). The parameters are periodicity constant g , length of square opening d and separation $2a$. (b) is 3-D view of (a). thickness t .

3.1.4.2 Experimental Results

Experiments were conducted on the meshes with rectangular arrangement of square openings at Naval Research Laboratory²⁶. Commercially prepared meshes²⁷ with 1000, 1500 and 2000 lines/inch were used. Transmittance through these meshes was calculated and is shown in Figure 3.5. Resonance and the Wave guide Modes were observed for each mesh. The geometrical parameters of these meshes are much smaller than what has been used for the simulations. All the meshes have a diameter of $4 \mu\text{m}$. For a mesh of 2000 lines/inch, periodicity constant ' g ' is calculated to be $12.7 \mu\text{m}$ and with the square opening of 0.0003inch ' d ' is calculated to be $7.62 \mu\text{m}$, but the assignment of the peaks is similar to the simulated results. It can be seen from Figure 3.5 that the wave guide mode appears close to the periodicity constant, the same value observed with the simulated results below. Similar is the case with 1000 and 1500 lines per inch.

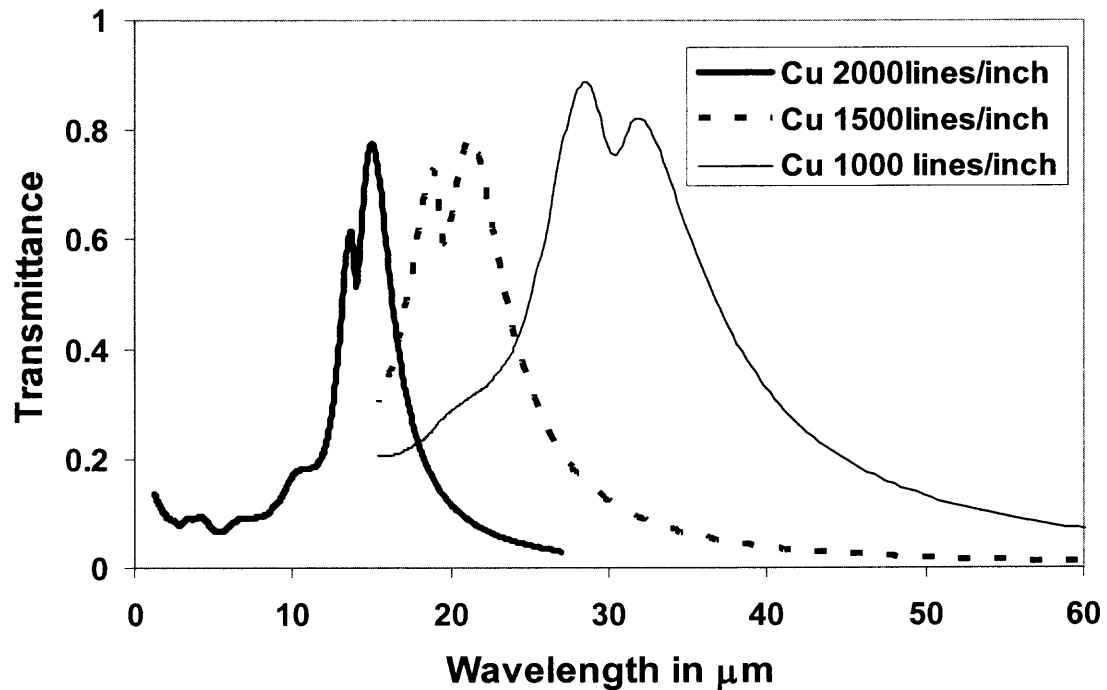


Figure 3.5 Experimental transmittance of Square meshes with 1000, 1500 and 2000 lines/inch.

3.1.4.3 Fixed Thickness and Varying Opening

The transmittance in meshes

with square shaped opening is shown in Figure 3.6 and is discussed by comparing it with the cross shaped opening in section 3.1.3. The width of the resonance mode is broader and the interaction between the resonance mode and the wave guide mode is less as compared to that of crosses. The wave guide mode appears as a shoulder and has a normalized wavelength of 1. Similar to the crosses, the resonance wavelength increases with the opening. It is observed that the bandwidth of the resonance mode and the transmission intensity are higher than that of the cross shaped openings. The bandwidth observed is 40% range with transmission intensity of 90%. Due to high transmission in the diffraction region, this filter is not preferred for filter applications.

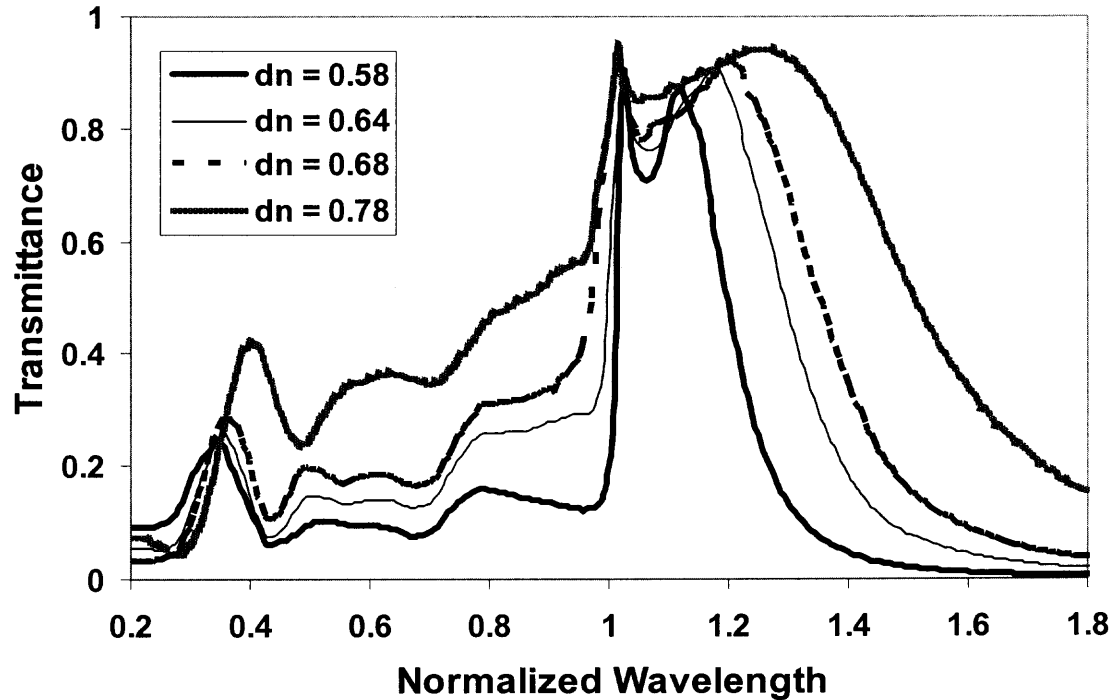


Figure 3.6 Square shaped opening in a rectangular mesh with fixed thickness of 0.43g and varying opening.

3.1.4.4 Fixed Opening and Varying Thickness With increase in thickness of the square shaped opening mesh, the resonance mode shifts to a higher wavelength as shown in Figure 3.7. The wave guide mode appears at normalized wavelength of 1 and remains at 1 for all thicknesses. The diffraction region i.e. the region of normalized wavelength, less than 1, shows a high transmission which is not desirable for an ideal filter.

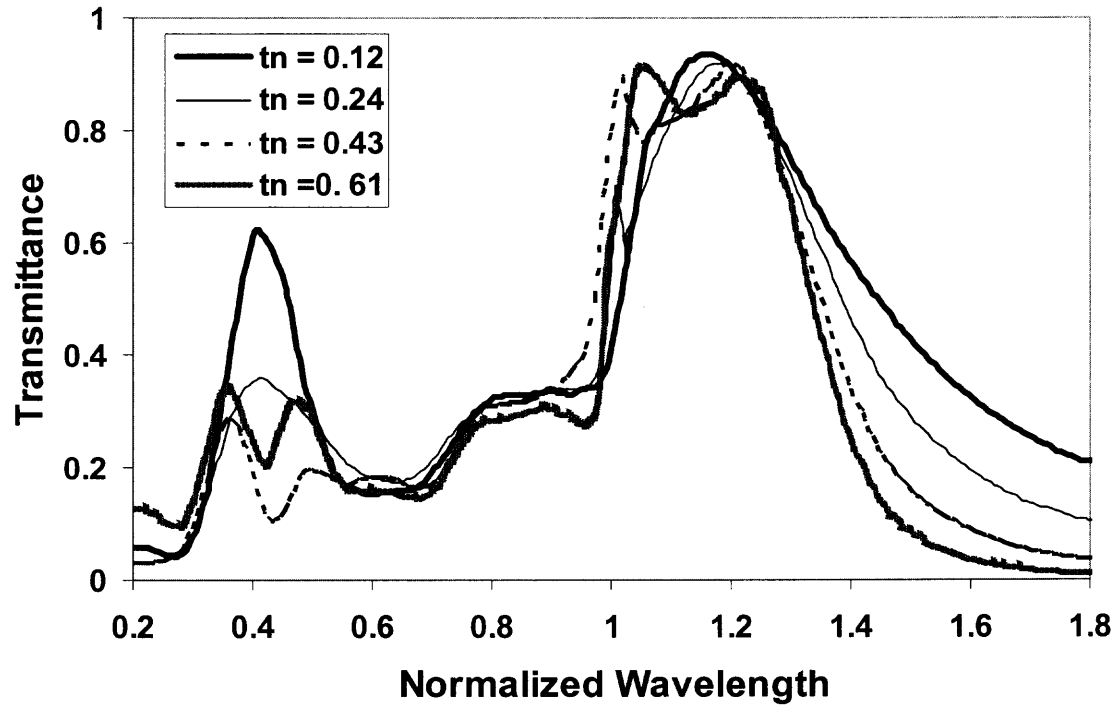


Figure 3.7 Square shaped opening in a rectangular mesh with fixed opening of $0.68g$ and varying thickness.

3.1.5 Rectangular Arrangement with Circular Shape Opening

3.1.5.1 Geometrical Parameters

Meshes with circular openings have been experimentally investigated²⁸. Figure 3.8(a) illustrates the 2D view of the mesh, where black is metal and white circles are the openings. ‘ d ’ is the diameter of the openings and ‘ g ’ is the periodicity constant. 3D view of the same structure can be seen in Figure 3.8(b) which the parameter thickness ‘ t ’ of the mesh is along the z direction.

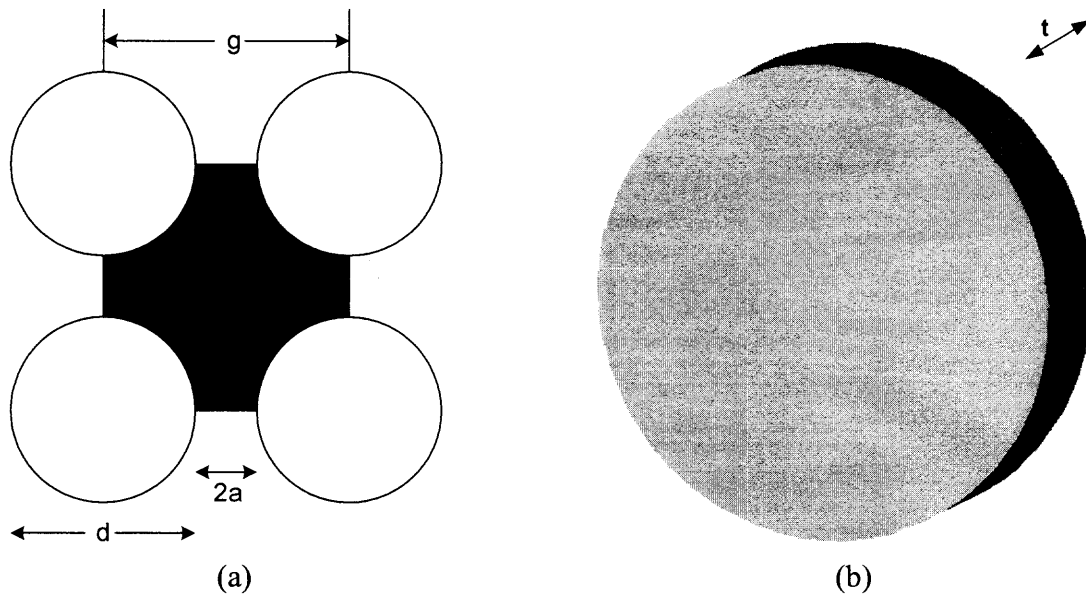


Figure 3.8 Rectangular arrangement of circular openings. Black is metal and White is opening in (a). The parameters are periodicity constant g , circle diameter d and separation $2a$. (b) is 3-D view of (a). thickness t .

3.1.5.2 Experimental Results

Transmittance of circular meshes has been measured in the shorter wavelength region³ and the experimental result is shown in Figure 3.9. The parameters used were diameter $d = 400$ nm, lattice constant $a = 750$ nm and thickness $t = 300$ nm. As will be seen later there is an agreement between the long wavelength simulations and the short wavelength experiments. In the experimental results, the mesh thickness was not thick enough to show the wave guide mode.

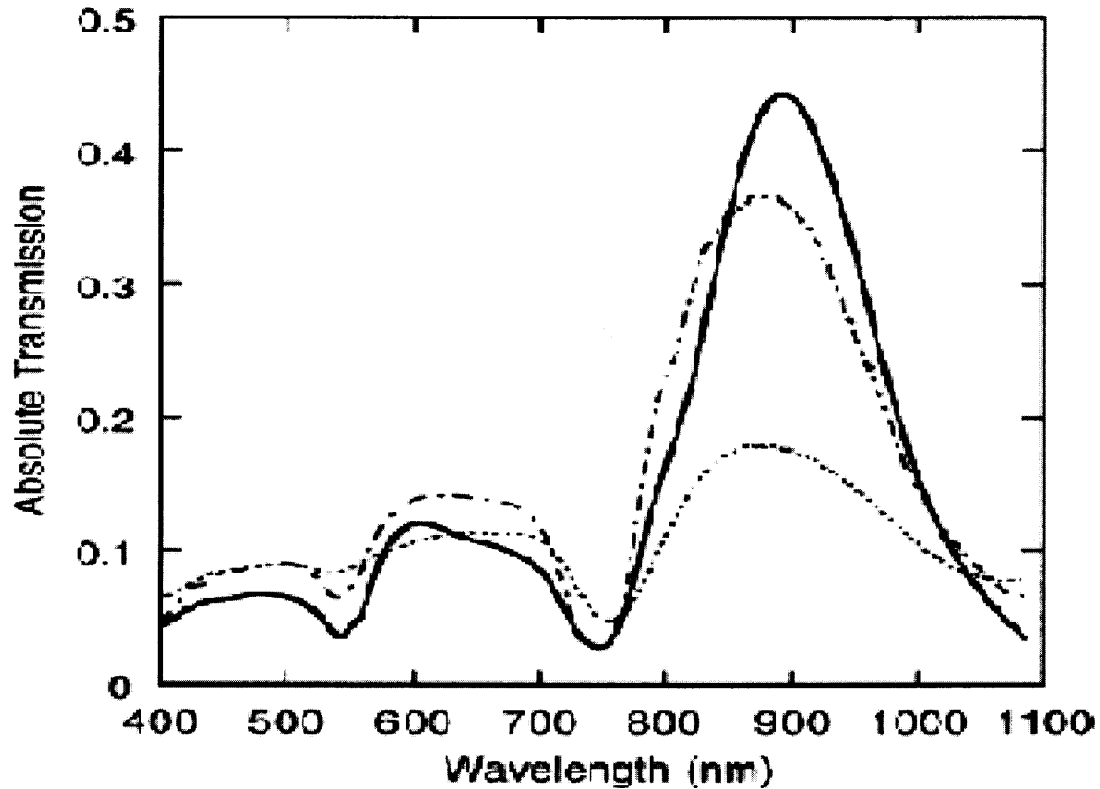


Figure 3.9 Transmission spectra of a circular mesh investigated experimentally²⁸ in the nm region. The inset shows the cross section of the film, White is Ag film, White and black is Ni film coated with Ag and Black is Ni film.

It can be observed from the above result that the simulation result with parameters $d_n = 0.58$ and $t_n = 0.43$ has similar result as will be seen in section below.

3.1.5.3 Fixed Thickness and Varying Openings

A similar effect of shifting of the resonance mode to higher wavelength is observed in the simulated results of circular openings as shown in Figure 3.10. The wave guide mode appears at normalized wavelength of 1. The minimum bandwidth achieved is about 10% and has a transmittance of around 80%. The diffraction region has a transmittance of around 20% or below.

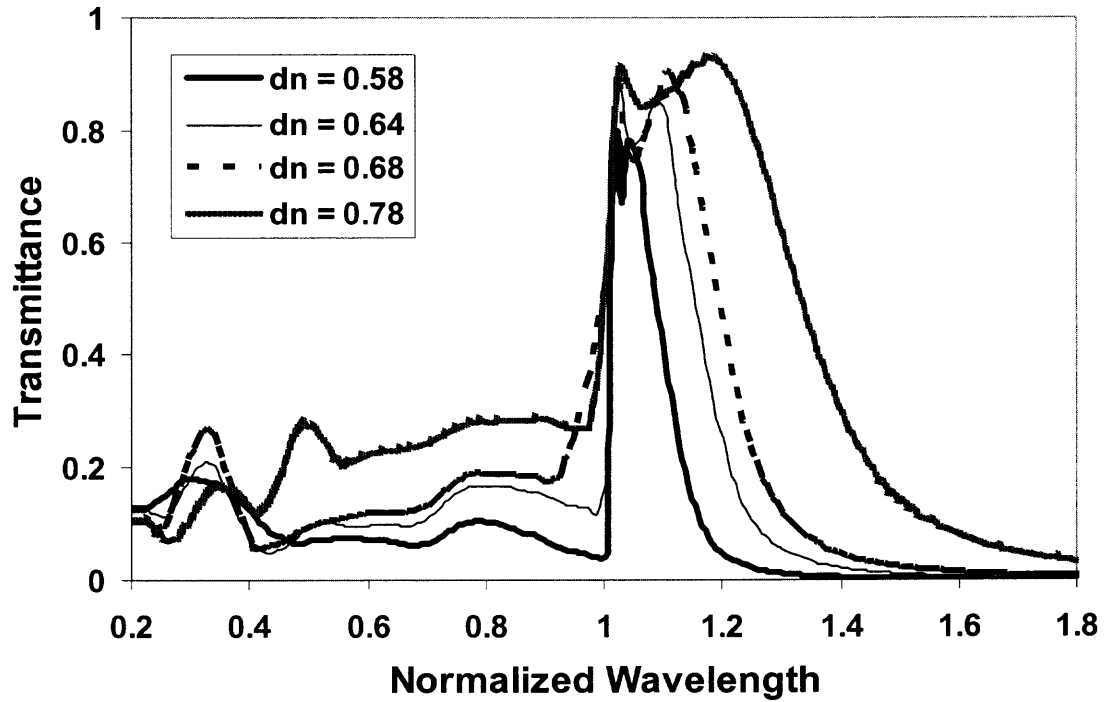


Figure 3.10 Circular shaped opening in a rectangular mesh with fixed thickness of 0.43g and varying opening.

3.1.5.4 Fixed Opening and Varying Thickness

The wave guide mode does not appear for thickness of $t_n = 0.12$ as can be seen in Figure 3.11. As t_n increases the wave guide mode begins to appear. It appears at normalized wavelength of 1. The resonance wavelength is approximately the same for all ' t_n '. The bandwidth is of the range of 25%. Transmittance in diffraction region is around 25% or less.

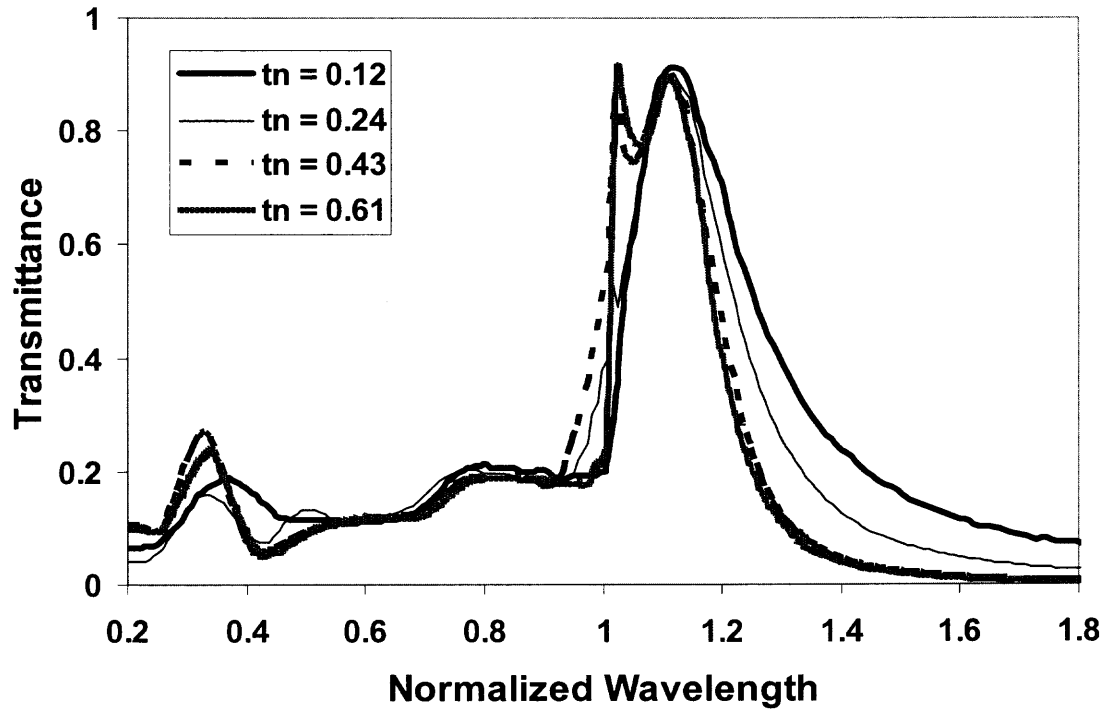


Figure 3.11 Circular shaped opening in a rectangular mesh with fixed opening of 0.68g and varying thickness.

Reducing the thickness will reduce the intensity of the wave guide mode and at lower thicknesses, the wave guide mode disappears. The intensity of the resonance mode can be increased by increasing the diameter of the openings but this increases the bandwidth of the wave. Hence a trade off is achieved to achieve the minimum bandwidth of 10% with maximum transmission intensity of 84% at $tn = 0.15$ and $dn = 0.68$ as shown below.

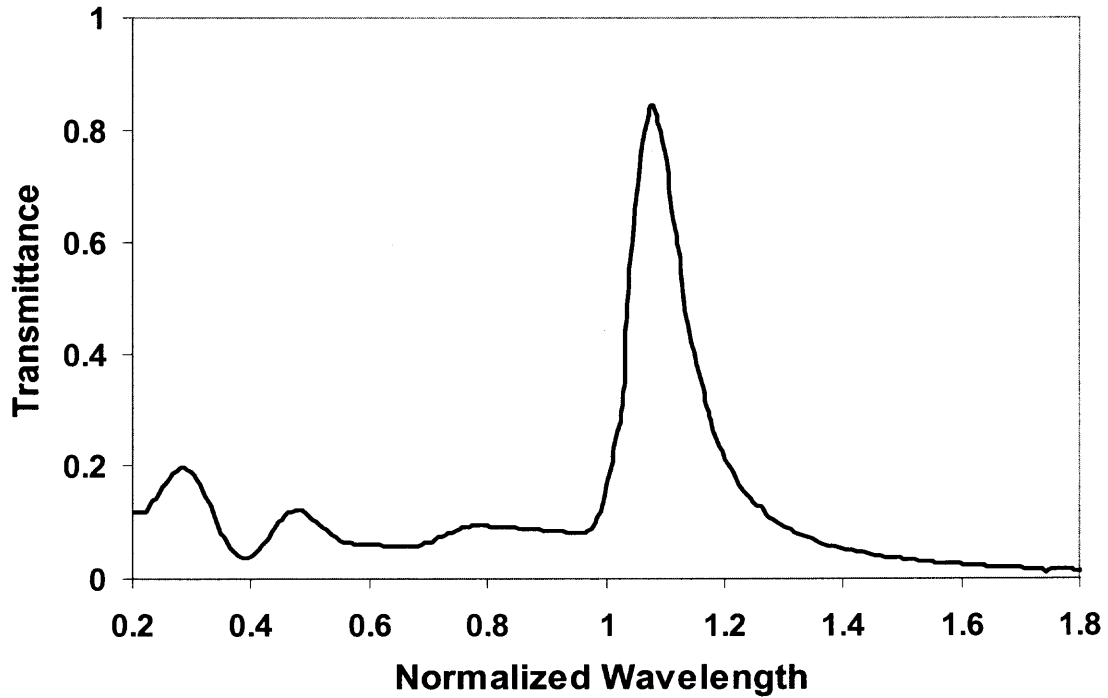


Figure 3.12 Circular shaped opening with 84% transmittance and a bandwidth of 10%.

3.1.6 Hexagonal Arrangement of Circular Shape Opening

Hexagonal arrangement of holes has been investigated experimentally by Huggard²⁹. Simulations using Micro-Stripes were performed on hexagonal arrangement of holes and the results are noted in the following sections.

3.1.6.1 Geometrical Parameters Hexagonal arrangement of holes has been investigated experimentally²⁹. Periodic arrangement of holes in hexagonal manner is shown in Figure 3.13. An additional periodicity constant ‘h’ needs to be defined for the hexagonal structure, see Figure 3.13(a), of magnitude $h = 0.87g$.

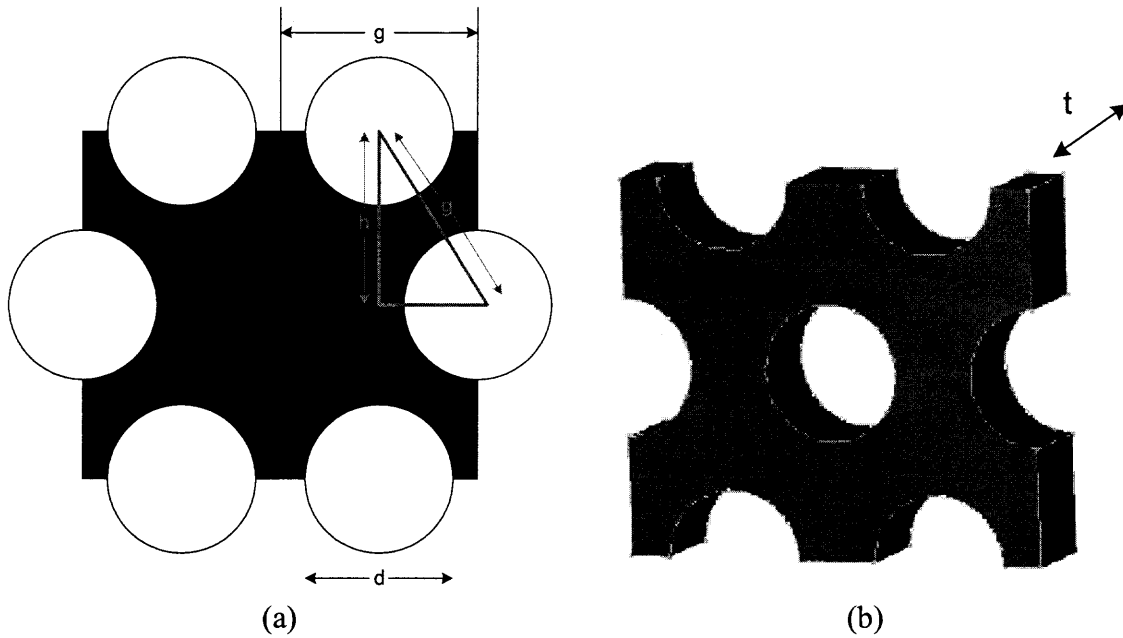


Figure 3.13 Hexagonal arrangement of circular openings. Black is metal and White is opening in (a). The parameters are periodicity constant g , circle diameter d (b) is 3-D view of (a). thickness t .

3.1.6.2 Experimental Results

An experimental result for similar hexagonal arrangement of holes is shown in Figure 3.14. As will be seen in section 3.1.5.3, this result matches with the simulation results. The wavelength is mentioned in cm^{-1} while the simulation results appear in normalized wavelength.

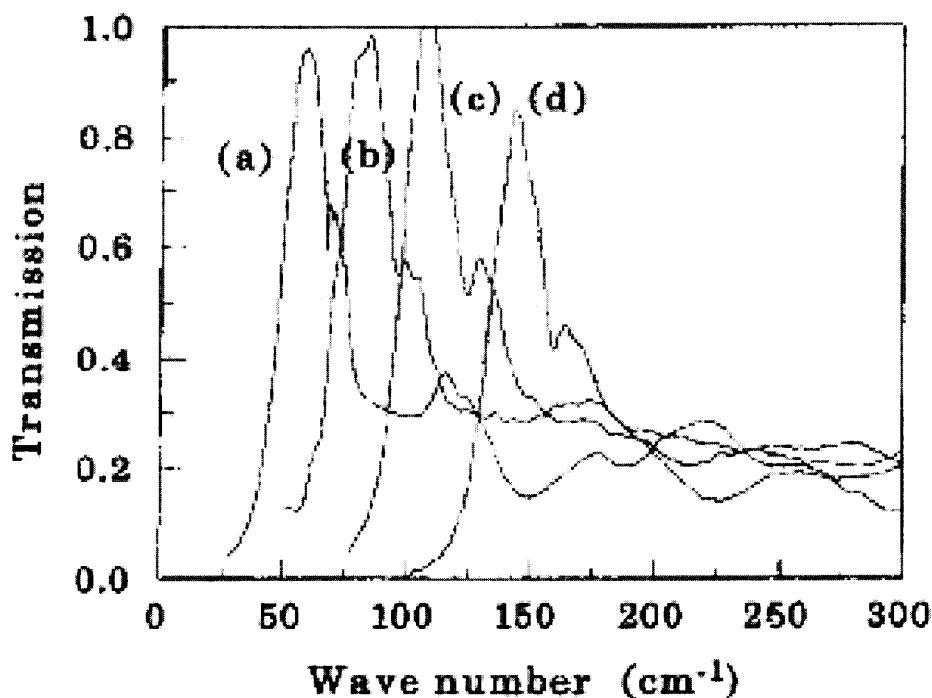


Figure 3.14 Experimental hexagonal shaped mesh with various opening⁵. The resonance and wave guide mode are clearly seen.

3.1.6.3 Fixed Thickness and Varying Openings

As observed from Figure 3.15, the wave guide mode appears at shorter wavelength as compared to the rectangular arrangements observed and explained above. It appears at $0.85g$ which is approximately equal to 'h', the smaller of the two periodicity constants. The resonance wavelength shifts to higher wavelength with increase in openings. The bandwidth of single peak is about 10% and transmission of about 80%. Transmission in the diffraction region is higher as compared to the experimental data, see Figure 3.14, but the Micro-Stripes program is limited in the diffraction region only to qualitative results.

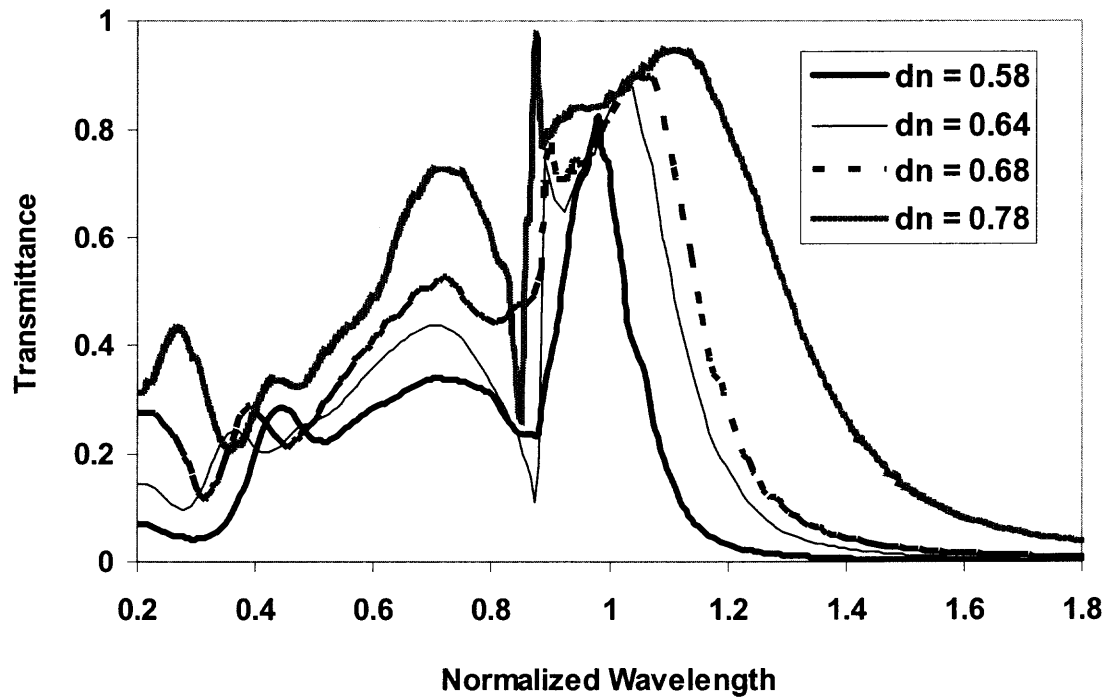


Figure 3.15 Hexagonal arrangement of holes with fixed thickness of $0.43g$ and varying opening.

3.1.6.4 Fixed Opening and Varying Thickness

The wave guide mode appears at $0.85g$ approximately equal to 'h'. The transmission intensity of resonance mode reduces with increase in thickness.

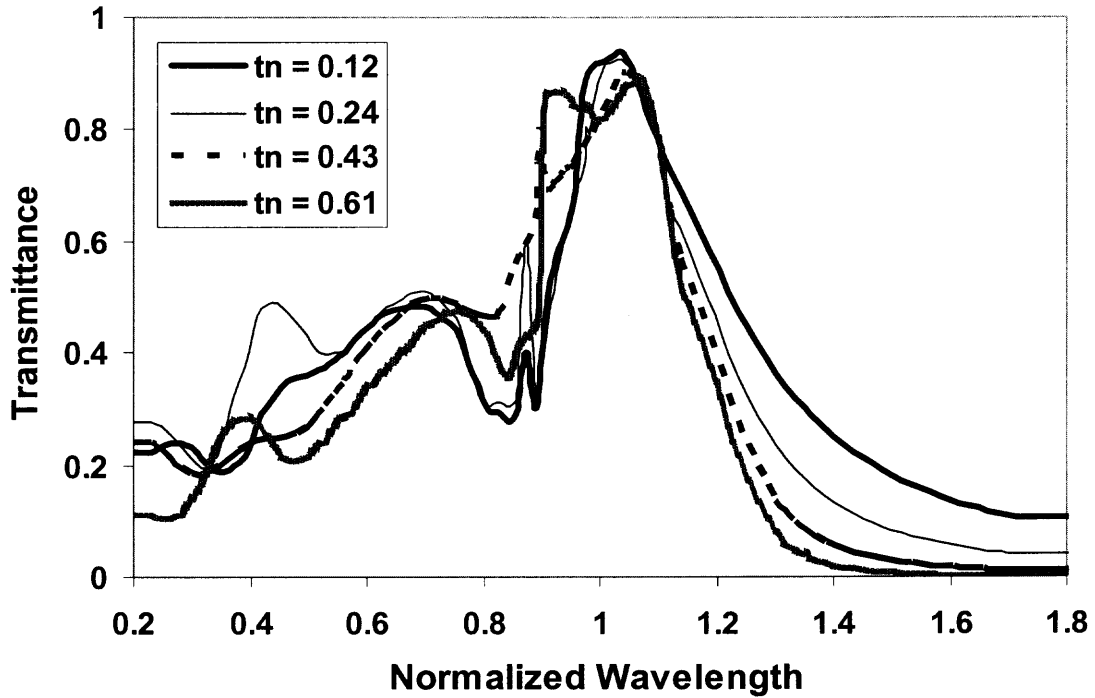


Figure 3.16 Hexagonal arrangement of holes with fixed opening of $0.68g$ and varying thickness.

3.1.7 Summary

The calculations show that the surface wave resonance appears for the rectangular structures of cross, square and circular shaped openings in the range of λ/g from 1.15 to 1.3 while for hexagonal structure it appears at 1 and smaller values. The surface wave resonance depends almost linearly on the diameter of the openings and has almost the same value for different thicknesses. For rectangular cross shaped opening, because of the interaction between the resonance and the wave guide mode, the dependence deviates from linearity.

The wave guide modes for rectangular cross, square and circular shaped openings are at normalized wavelength 1, while for hexagonal structure it appears at shorter wavelength, corresponding to the smaller of the two lattice vectors. The transmission

intensity increases with the size of the openings and for the rectangular cross shaped mesh, there is an interaction of resonance and wave guide mode.

In the diffraction region, for wavelength smaller than g , rectangular cross structures have the smallest transmittance of less than 10%, the rectangular circular structures has about less than 20% and the other structures have higher transmittance making the cross and circular structures preferable for filter design. Figure 2.17 shows the transmittance of circular, square and hexagonal meshes ($d_n = 0.58$ and $t_n = 0.43$) and it is observed that the most narrow shape is observed from the rectangular circular structure with a bandwidth of about 10%.

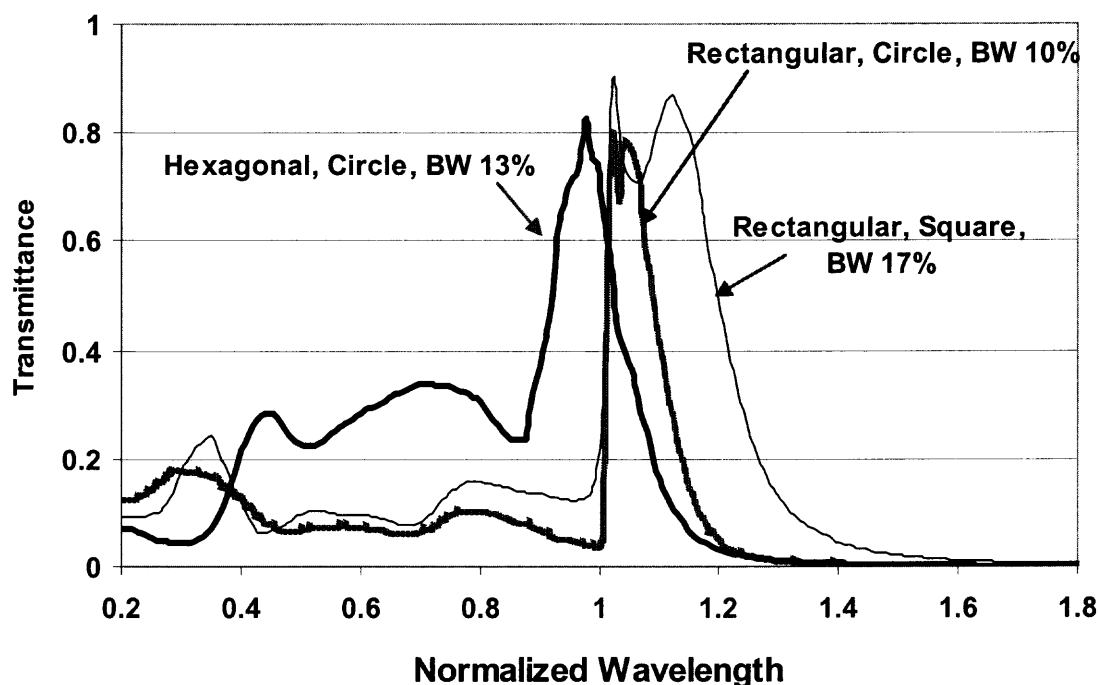


Figure 3.17 A specific case of 3 shapes, hexagonal, circular and square type mesh. The specifications for the 3 meshes are $d_n = 0.58$ and $t_n = 0.43$.

3.2 Photonic Double Layer of Thick Cross Shaped Inductive Meshes

Thick cross shaped metal meshes show resonance and wave guide mode. The resonance mode depends on the geometrical shape and size of the openings, but not much on the thickness of the mesh, while the wave guide modes depend little on the shape and size of the openings, but much on the thickness of the mesh. Two meshes in the Photonic crystal configuration require that the crosses of the two meshes are aligned, see Figure 3.18.

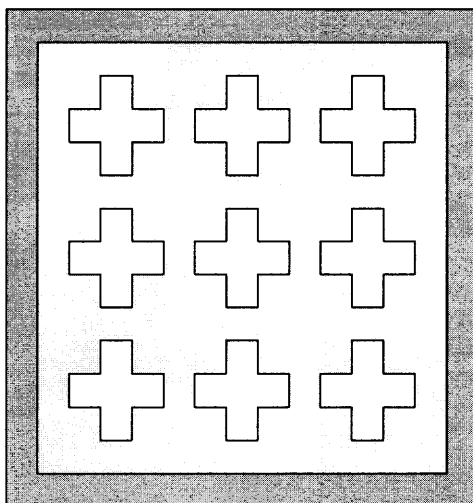


Figure 3.18 Two cross-shaped Inductive aligned meshes.

In addition to the resonance and wave guide mode, the separation of the two meshes will show a third type of mode, the stacking modes, depending on the separation of the meshes, Figure 3.19. These modes are different from “Fabry Perot” modes, as observed when using two non periodic reflecting plates. The meshes may be considered as oscillators and the stacking mode, at distances depending on the wavelength of the resonance modes, is generated by the interaction of the meshes.

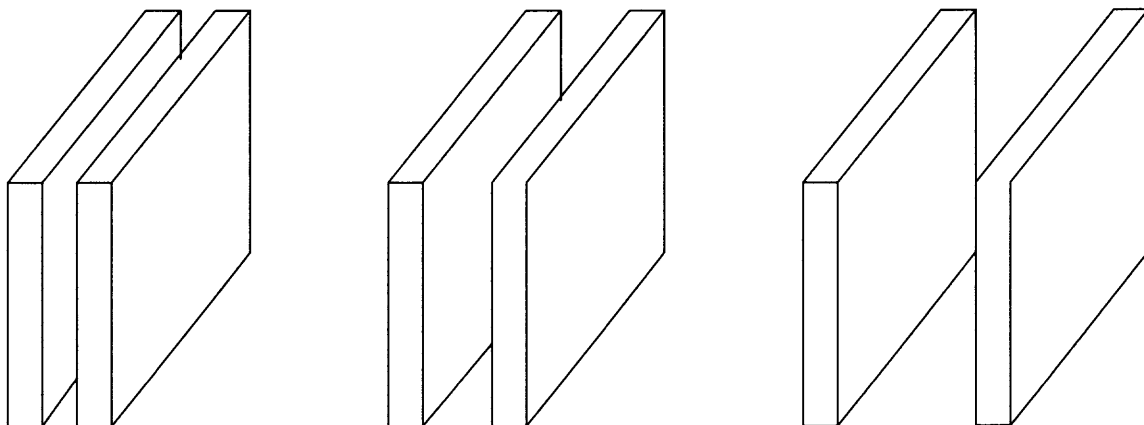


Figure 3.19 Schematic of two aligned meshes at various separations.

3.2.1 Two $2\mu\text{m}$ Thick Meshes

The Transmittance of two cross shaped meshes of thickness $2\mu\text{m}$ at separations 1, 3, 4, 7, and $11\mu\text{m}$ is shown in Figure 3.20. At separation of $1\mu\text{m}$ the resonance of the meshes appears as one peak of wavelength $31\mu\text{m}$, with peak transmission intensity of about 65%.

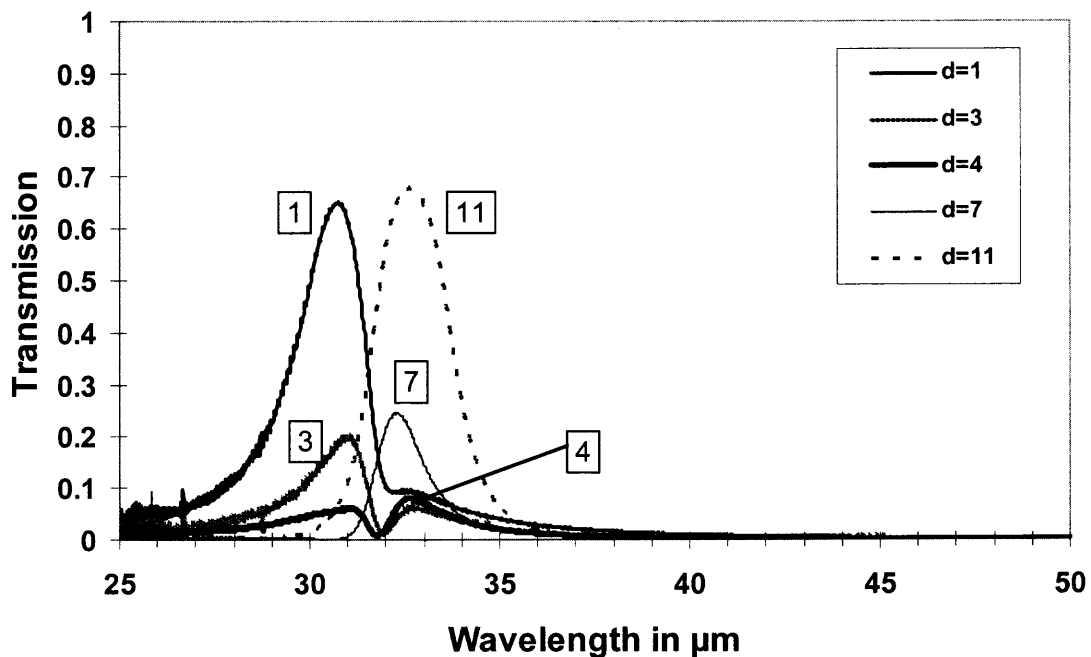


Figure 3.20 Transmittance of two thin metal meshes of thickness $2\mu\text{m}$ at separations 1, 3, 4, 7, 9 and $11\mu\text{m}$.

Further separation to $4\mu\text{m}$ reduces the intensity to less than 10%. As the separation increases, a shifted resonance peak appears at $34\mu\text{m}$.

3.2.2 Two $4\mu\text{m}$ Thick Meshes

The transmittance of two cross shaped meshes of thickness $4\mu\text{m}$ at separations 1, 4, 5, 6, 9 and $12\mu\text{m}$ is shown in Figure 3.21. At separation of $1\mu\text{m}$, the peaks of the two resonances appear separately, and at separation of $4\mu\text{m}$ together, at a peak of width 10% and transmission intensity of 95%. At this fixed spacing, the two meshes may be used as a narrow band pass filter.

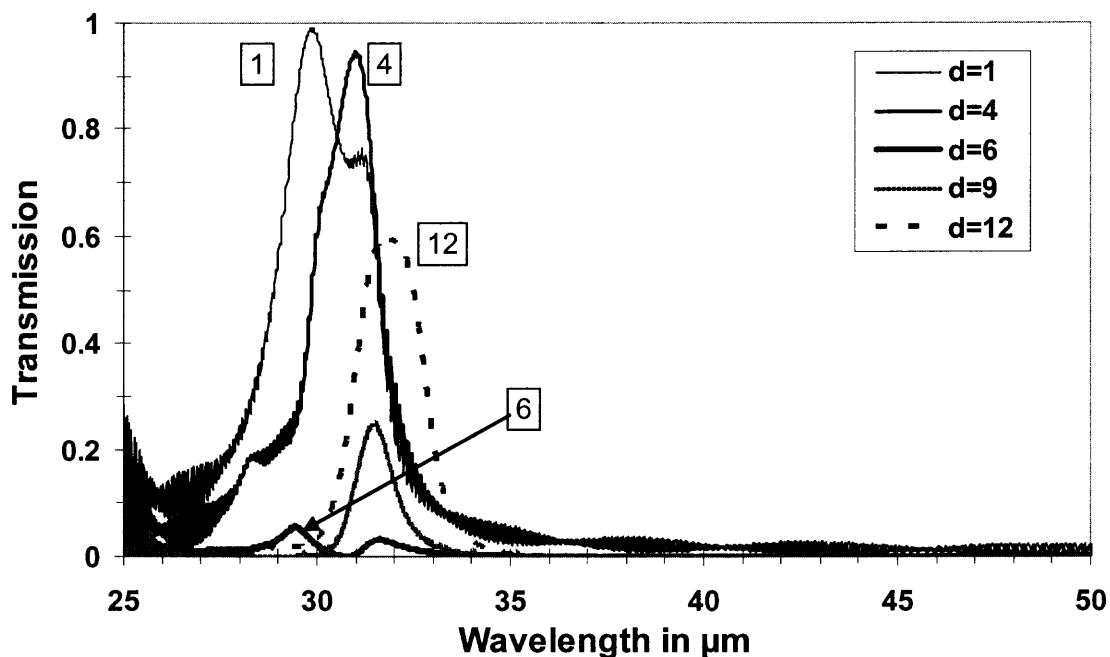


Figure 3.21 Transmittance of two thin metal meshes of thickness $4\mu\text{m}$ at separations 1, 4, 5, 6, 9 and $12\mu\text{m}$.

When changing the separation further, from 4 to $6\mu\text{m}$, the resonance wavelength peak at $31\mu\text{m}$, with peak intensity of about 95%, is dramatically reduced to an intensity

of about 5%. Increase in the separation will produce a shifted resonance peak at $32\mu\text{m}$ of 60% transmission. By changing only the separation by $2\mu\text{m}$, maybe with a piezo-electric crystal, one could use these meshes for a switch or modulator.

3.2.3 Two $11\mu\text{m}$ Thick Meshes

The Transmittance of two cross shaped meshes of thickness $11\mu\text{m}$ separated by $4\mu\text{m}$ and $8\mu\text{m}$ is shown in Figure 3.22. At $8\mu\text{m}$, which is in the range of a quarter wavelength of the resonance wavelength of both meshes, there is almost no transmittance.

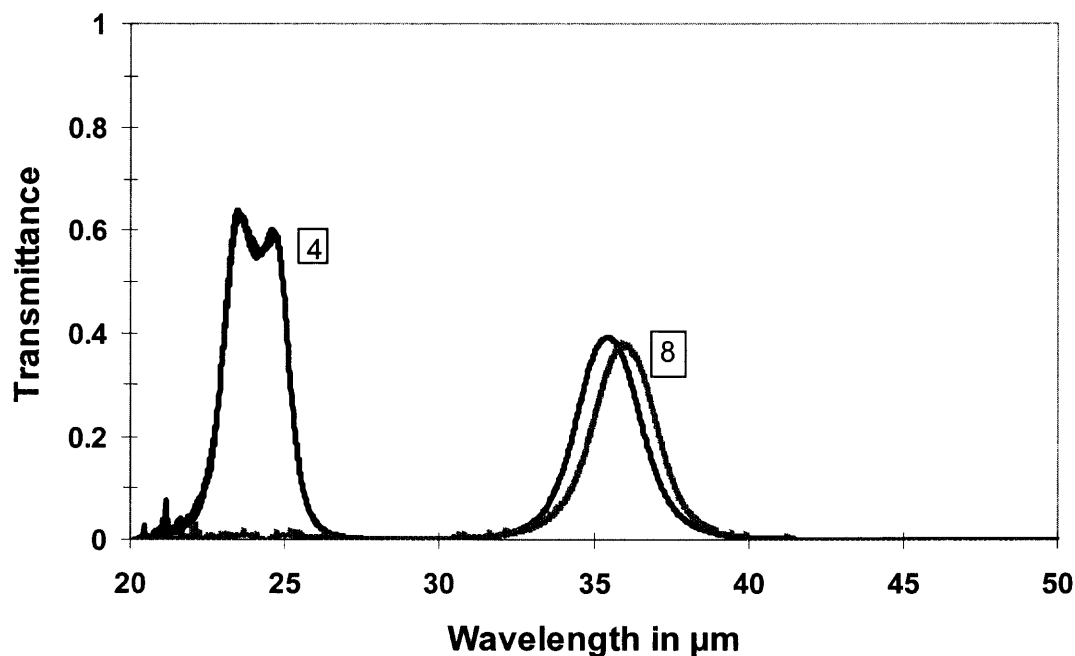


Figure 3.22 Transmittance of cross shaped meshes of thickness $11\mu\text{m}$ at separations of $4\mu\text{m}$ and $8\mu\text{m}$. The peak at around $36\mu\text{m}$ is the resonance wavelength of the meshes.

With a change in separation of $4\mu\text{m}$ almost all intensity is reduced to zero over an extended spectral range of 20 to $30\mu\text{m}$. These thicker meshes may have an advantage

from the point of view of mechanical strength and parallel surfaces for application for a switch or modulator.

3.2.4 Two 5.5 μm Thick Meshes as Tunable Filters

3.2.4.1 Wave Guide Modes

The transmittance of two cross shaped meshes of thickness 5.5 μm at separations of 0.4, 1, 2, 3, 4 and 5 μm is shown in Figures 3.23 and 3.24. The peaks correspond to wave guide modes and cover the spectral range from 21 μm to 25 μm . With a band pass filter of bandwidth of 15 to 20% and a piezo-electric crystal, one could operate the two meshes as a tunable filter.

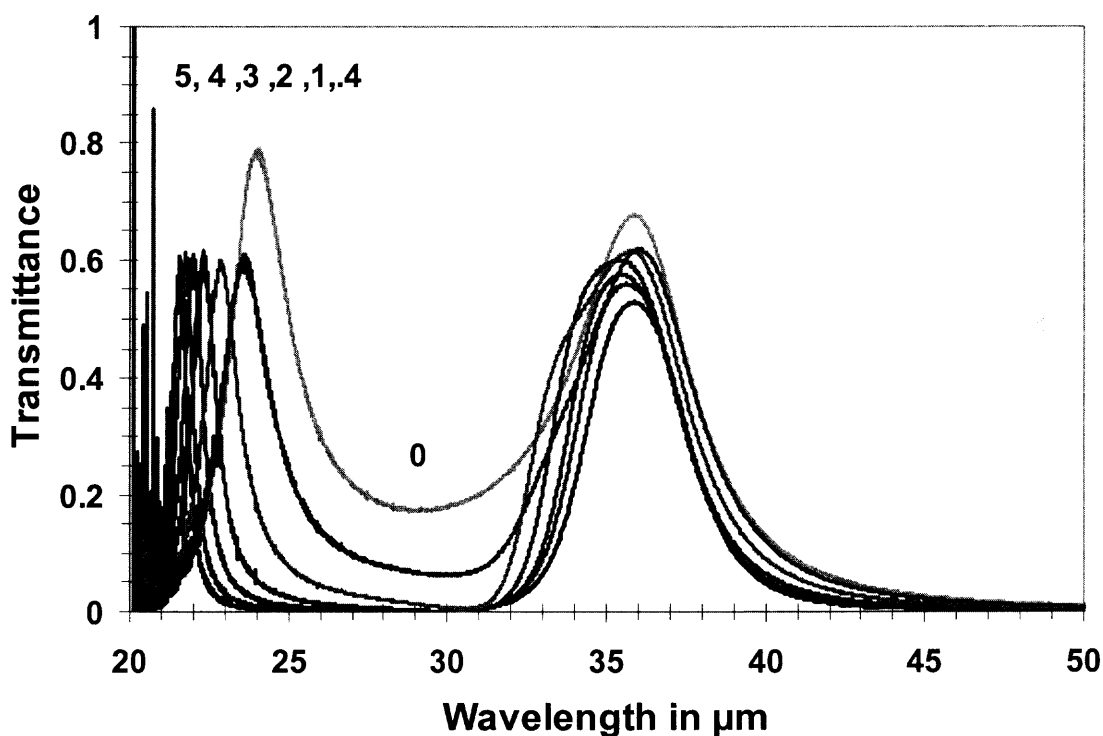


Figure 3.23 Transmittance of two meshes of thickness 5.5 μm at separations of 0.4, 1, 2, 3, 4 and 5 μm .

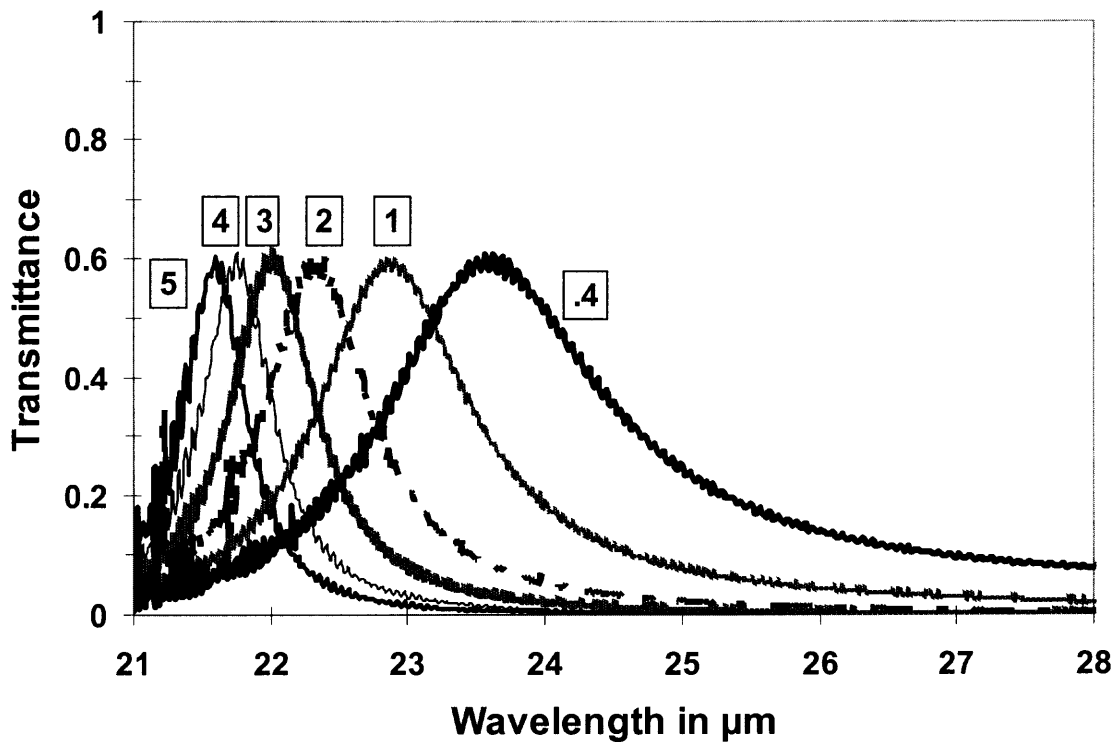


Figure 3.24 Expanded plot of section for separation of 0.4, 1, 2, 3, 4 and 5 μm .

3.2.4.2 Stacking Modes

The transmittance of two cross shaped meshes of thickness 5.5 μm at separations 11 to 16 μm is shown in Figure 3.25. The modes are stacking modes and to be operated as tunable filter, a band pass filter of 40% band width is needed.

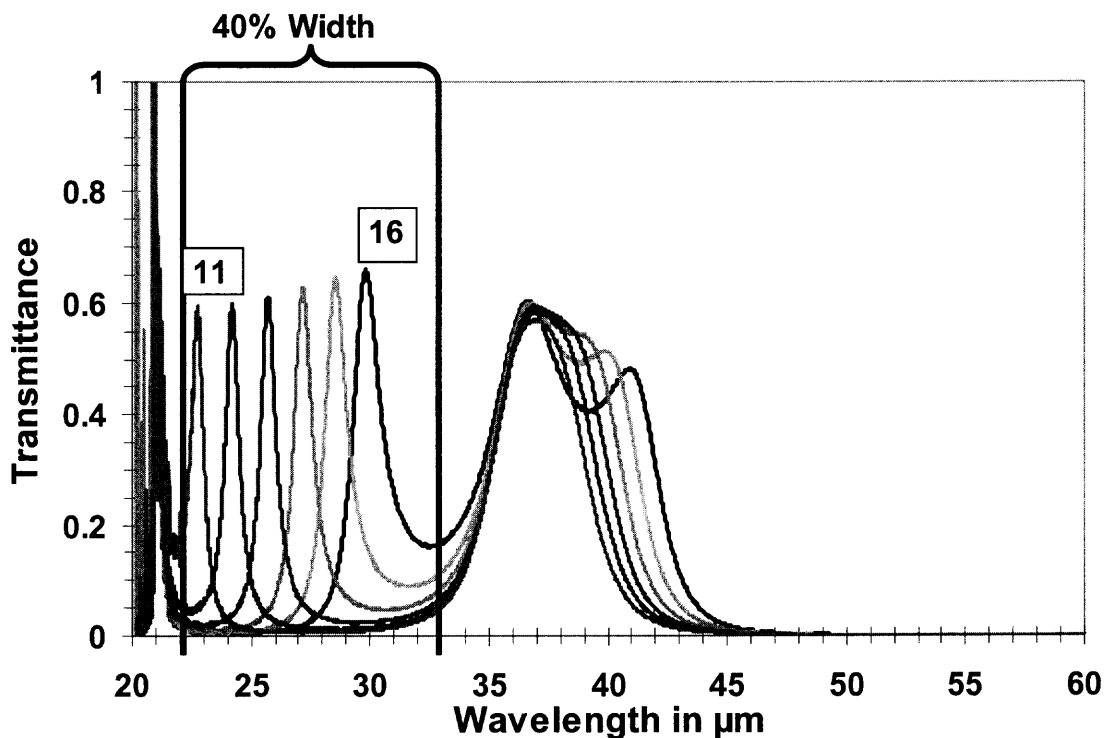


Figure 3.25 Transmittance of two meshes of thickness $5.5\mu\text{m}$ and separation of 11, 12, 13, 14, 15, $16\mu\text{m}$.

3.2.5 Summary

The meshes of thickness $2\mu\text{m}$ and $4\mu\text{m}$ can be produced with the photoresist method and electroforming process, while the mesh of thickness $5.5\mu\text{m}$ and thicker would need the LIGA method for fabrication. Such meshes may be produced of size 20mm by 20mm as free standing meshes. The movement of a few microns of one mesh with respect to the other may be done with a piezoelectric crystal. When using nickel meshes, a magnetic field may be employed. These two mesh layers may be used as switches in a specific spectral region in conjunction with a suitable band pass filter as tunable filters.

3.3 Metallodielectric Photonic Crystals

Stacks of inductive metal meshes were used to develop Metallodielectric Photonic Crystals (MPC). An arrangement of metal spheres in the form of Cubic, Body Centered Cubic (BCC) and Face Centered Cubic (FCC) Photonic Crystal (PC) as shown in Figure 3.26 were investigated by simulations. Metal spheres are placed in stacks forming a layered structure. The crystal parameters are the diameter of the sphere 'd', the crystal lattice constant 'a', that is the center to center distance between two adjacent spheres, and the separation 's' between consecutive layers. Periodicity constant is the shortest distance between the two spheres. The layers are separated by a dielectric medium with dielectric constant close to air. These parameters along with the number of layers are varied for sphere arrangements, and reflection peaks are recorded for normal incidence light. The selected frequency range from 5 GHz to 30 GHz correspond to a range of wavelength from 10 mm to 60 mm. The reflection peaks are interpreted with two types of modes, the resonance mode of a single layer, corresponding to the resonance minimum of a capacitive mesh, and the resonance of the stacking modes, generated by the stack of equally spaced layers, corresponding to Bragg reflection¹⁶.

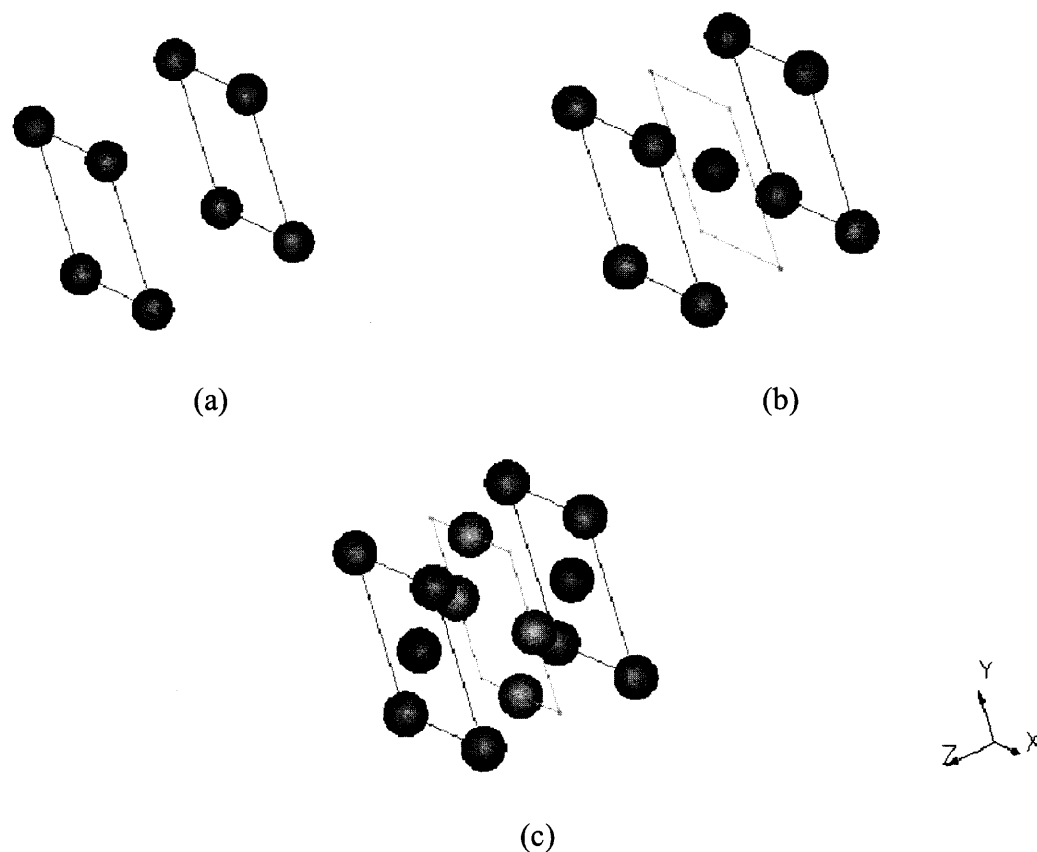


Figure 3.26 Two layers of Cubic Photonic Crystal (a); Three layers of Body Centered Cubic (BCC) (b); Three layers of Face Centered Cubic (FCC) (c).

3.3.1 Simple Cubic Photonic Crystals

The Micro-Stripes program allows the study of the layered arrangement of spheres. Figure 3.26(a) shows two layers of Simple Cubic PC. The unit studied with the Micro-Stripes program consists of four metal spheres. The lattice constant, that is the distance between adjacent spheres, was assumed 15 mm, the separation between layers 15 mm and the periodicity constant equal to the crystal lattice. Hence, two layers together make it a Simple Cubic structure. Simulations were performed and reflection peaks studied, depending on number of layers, sphere diameter 'd' and separation 's' between layer.

3.3.1.1 Dependence on Number of Layers

3.3.1.1.1 Transmission for Crystal Lattice of 15 mm

Figure 3.27 shows reflection peaks of a simple cubic structure with $a = 15$ mm, $d = 6.35$ mm and $s = 15$ mm. The periodicity constant is 15 mm. Starting with one layer, crystals are simulated with up to ten layers, and peaks are studied at normal incidence.

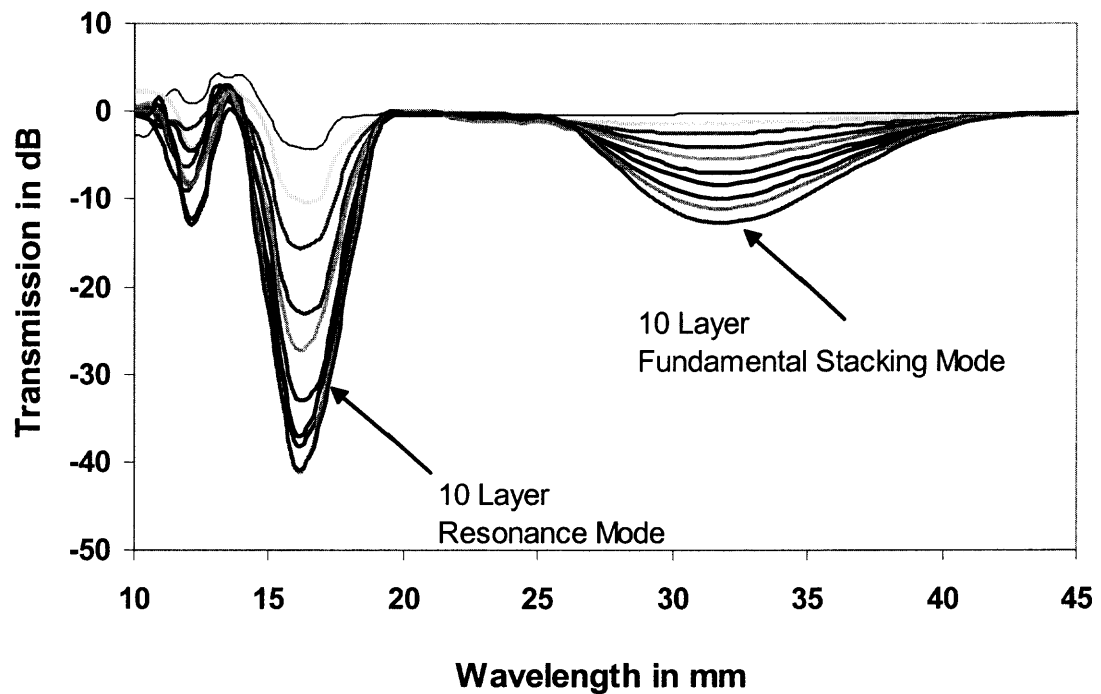


Figure 3.27 Micro-Stripes calculated transmission of a Cubic crystal with 1 to 10 stacked layers. The parameters of the crystal are $a = 15$ mm, $d = 6.35$ mm and $s = 15$ mm.

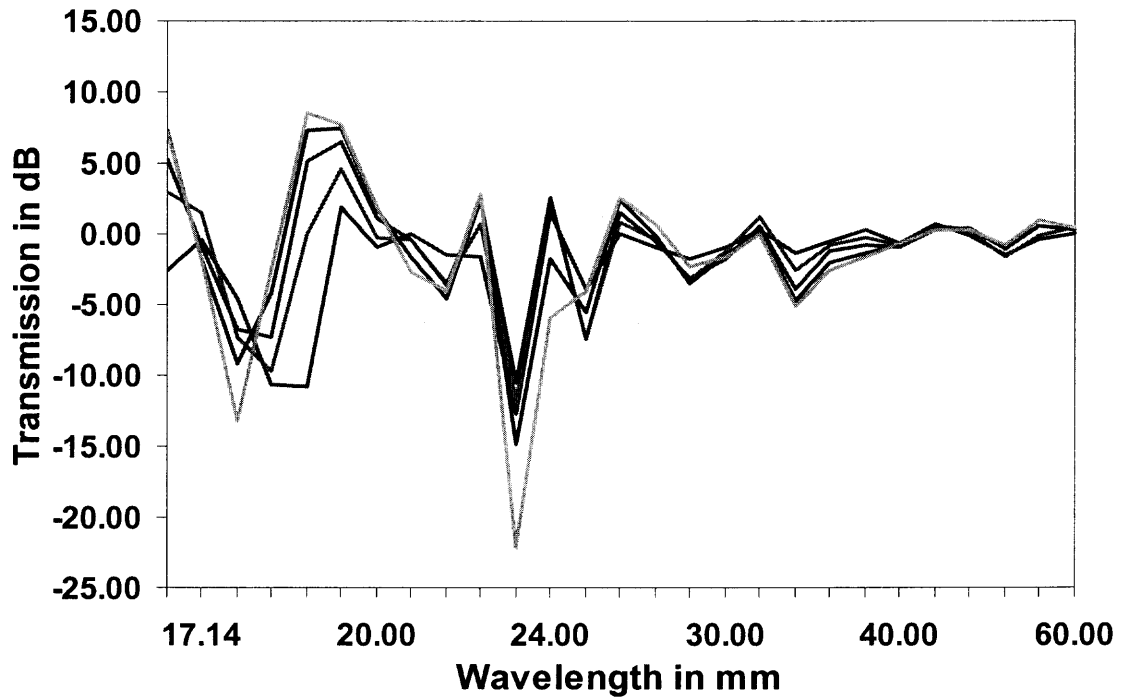


Figure 3.28 Micro-Stripes calculated transmission of a Cubic crystal with 1 to 10 stacked layers. The parameters of the crystal are $a = 15$ mm, $d = 6.35$ mm and $s = 15$ mm.

The resonance mode appears at 16 mm, the fundamental stacking mode at 32 mm, and therefore, the first order stacking mode is expected also at 16 mm. The wavelength of the resonance mode is expected around the lattice distance $a = 15$ mm, but due to the interaction of this mode with the first order stacking mode it appears at 16 mm. A higher order stacking mode can be seen at 12 mm. The intensity of the modes increases with increasing number of layers.

3.3.1.1.2 Transmission for Crystal Lattice of 20mm

For lattice distance of 20 mm, transmission was observed experimentally by J. Tobias¹⁷, see Figure 3.29 and compared with simulations. Number of layers is varied from 1 to 6. The other parameters are $d = 6.35$ mm, $a = 20$ mm and $s = 20$ mm. Periodicity constant is 20 mm.

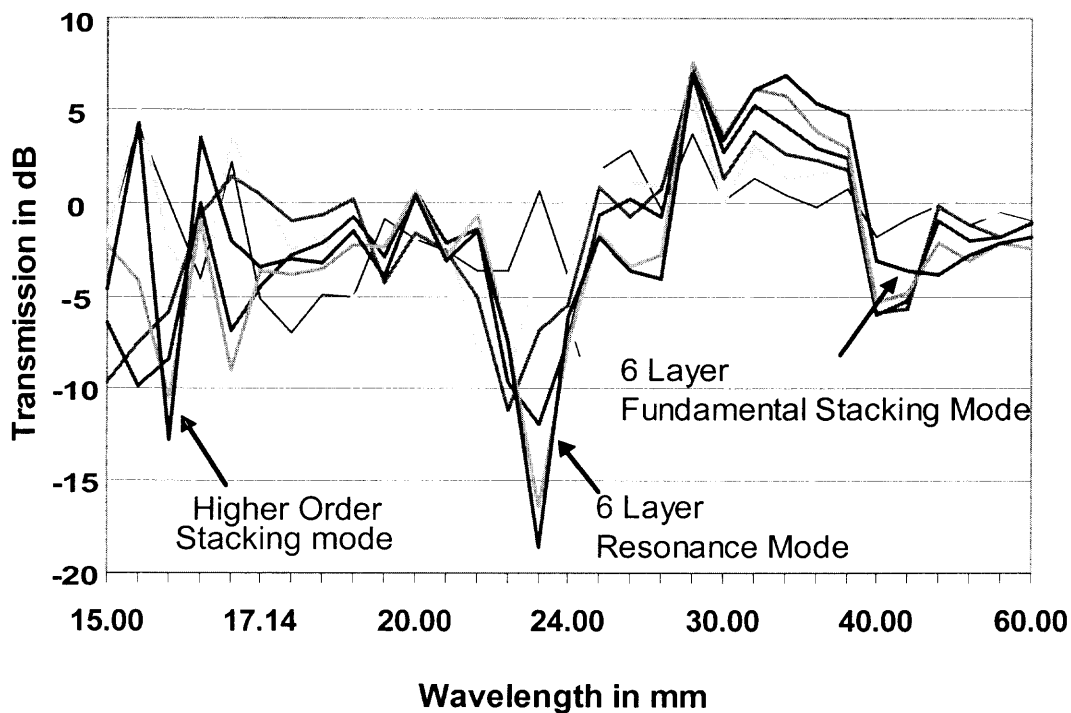


Figure 3.29 Experimental transmission of Simple Cubic crystal with crystal lattice $a = 20$ mm. The parameters of the crystal are $d = 6.35$ mm and $s = 20$ mm.

In Figure 3.30, simulations are shown for 1 to 6 layers. For six layers, the resonance mode appears at 22 mm and the fundamental stacking mode at 42.86 mm. The resonance mode is expected around 20 mm, but due to its interaction with the first order stacking mode, expected around 21 mm, it is shifted to longer wavelength. The second order stacking mode appears at 16 mm. The simulation results shown in the Figure 3.30 agree very well with the experimental results of Figure 3.29.

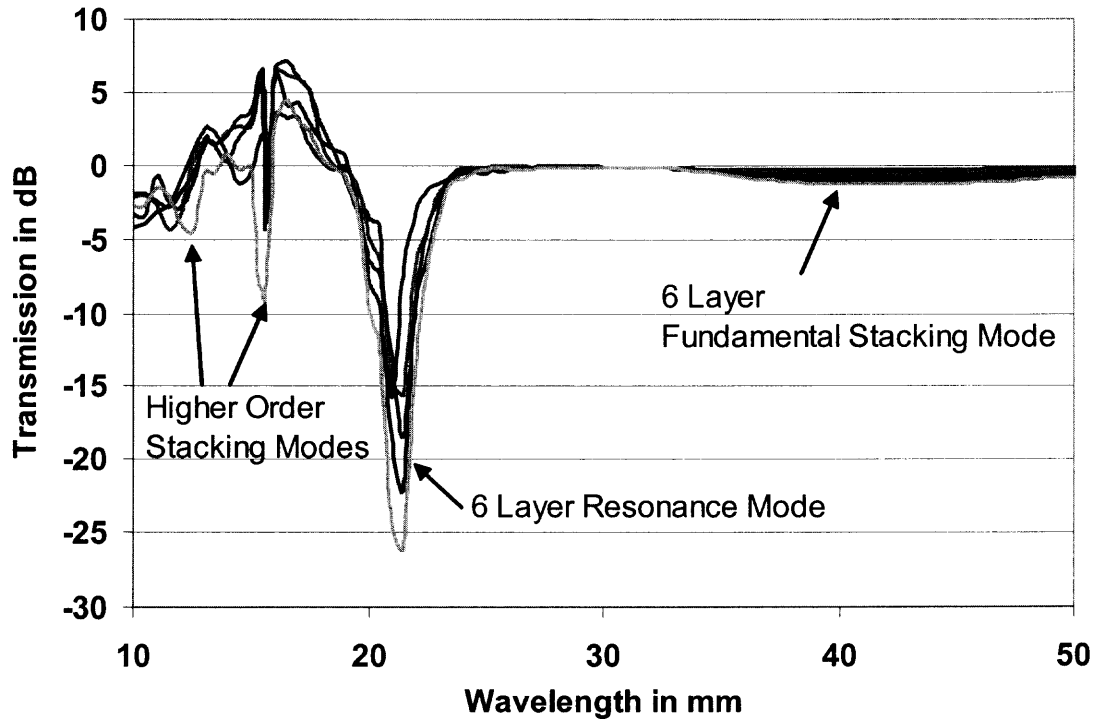


Figure 3.30 Micro-Stripes calculated Cubic crystal with crystal lattice $a = 20$ mm. The other parameters are $d = 6.35$ mm and $s = 20$ mm.

3.3.1.2 Dependence on Sphere Diameter 'd' Transmission through crystals for various sphere diameters 'd' is calculated and shown in Figure 3.31. The parameter 'd' is varied as 4, 6.35, 7 and 8 mm, with $a = 15$ mm and $s = 15$ mm, and simulations are performed for 10 layers. It is seen that as the amount of metal reduces, transmission increases. The effect of smaller sphere diameters of 4 and 6.35mm shows low interaction of the modes as compared to interaction in 7 and 8 mm. For smaller diameters of 4 and 6.35 mm, the first order stacking mode and the resonance mode overlap and increase in intensity as well as the fundamental stacking mode. For larger diameters, the resonance mode and the first order stacking mode appear separated with decreased intensity,

indicating stronger interaction, and the fundamental mode appears stronger and broader.

The second order stacking mode appears at the same position for all 'd'.

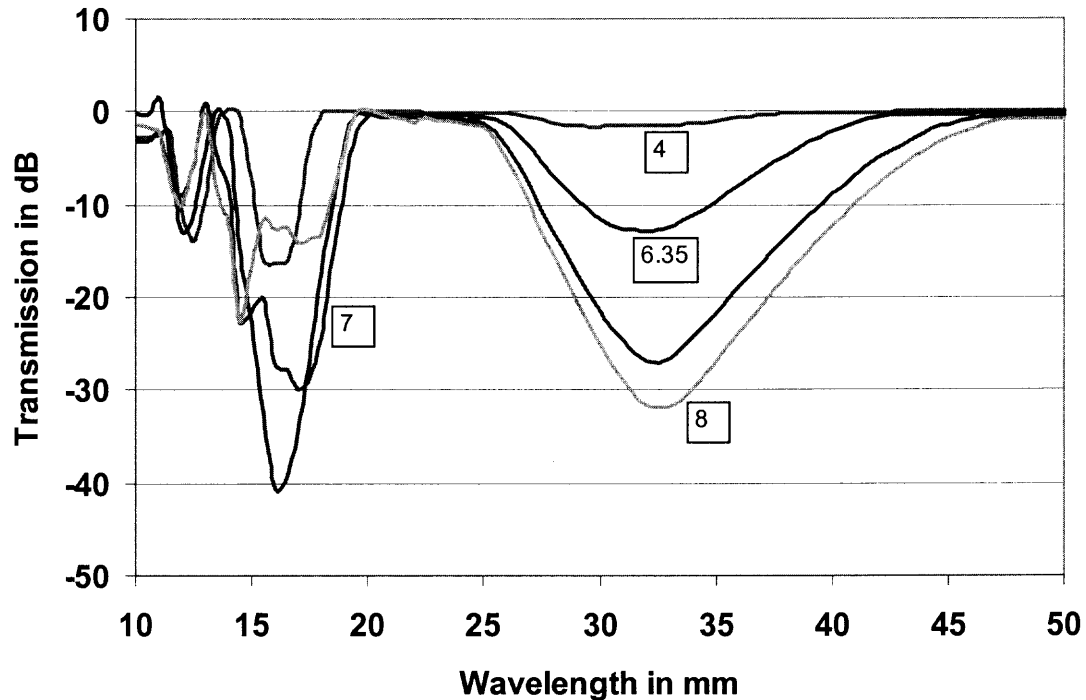


Figure 3.31 Transmission of Simple Cubic crystal depending on the sphere diameter $d = 4, 6.35, 7$ and 8 mm, $a = 15$ mm.

3.3.1.3 Dependence on Separation 's' of Layers

Separation between layers

plays a very important role in shifting the modes to longer wavelengths. Till now separation 's' of 15 mm was considered, which made the structure, a perfect Simple Cubic structure. Simulations for ten layers are performed for $a = 15$ mm, $d = 6.35$ mm and s is varied as 7.5, 15 and 20 mm. Separation of 7.5 mm gives an approximate BCC PC. This is because the second layer is not shifted in this case. Figure 3.32 shows the effect of separation on the mode wavelengths.

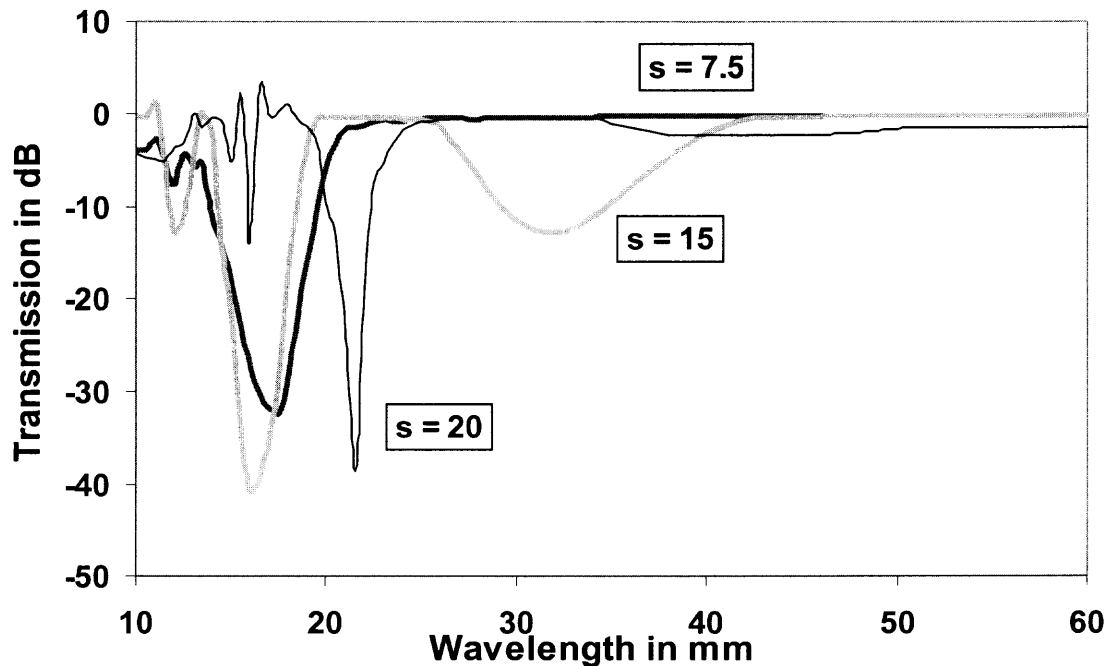


Figure 3.32 Transmission of Cubic crystal with Separation between the Stacking Layers 's' varied as 7.5, 15, and 20 mm. The other crystal parameters are $a = 15$ mm and $d = 6.35$ mm.

As observed in above section, the perfect Simple Cubic structure has the resonance mode at 16 mm, the fundamental stacking mode at 32 mm, the first order stacking mode at 16 mm and the second order stacking mode at 12 mm. The resonance mode and first order stacking mode overlap. For $s = 7.5$ mm, the resonance mode at 16 mm and the fundamental stacking mode, now also at 16mm, overlap and hence this mode is shifted further to 17.5 mm. This effect is similar to BCC with slight modification which will be seen later in section 3.3.2 of this chapter. For $s = 15$ mm, the resonance mode shifts to 16mm, that is to shorter wavelength, and for $s = 21.5$ mm to longer wavelength, with respect to the value for $s = 7.5$.

3.3.1.4 Transmission Line Theory

The interaction between resonance and stacking mode is also calculated with Transmission Line Theory. This theory does not account for the fact that the second layer for any of the crystal arrangement is shifted or not shifted. The resonance mode corresponds to an oscillator of resonance wavelength λ_R , presented by the impedance of a capacitive mesh, and the stacking modes resonance is depending on the spacing between the layers. Assuming resonance wavelength of 16mm corresponding to the periodicity constant of 15 mm, and assuming for the number of layers 6, all reflection peaks are plotted.

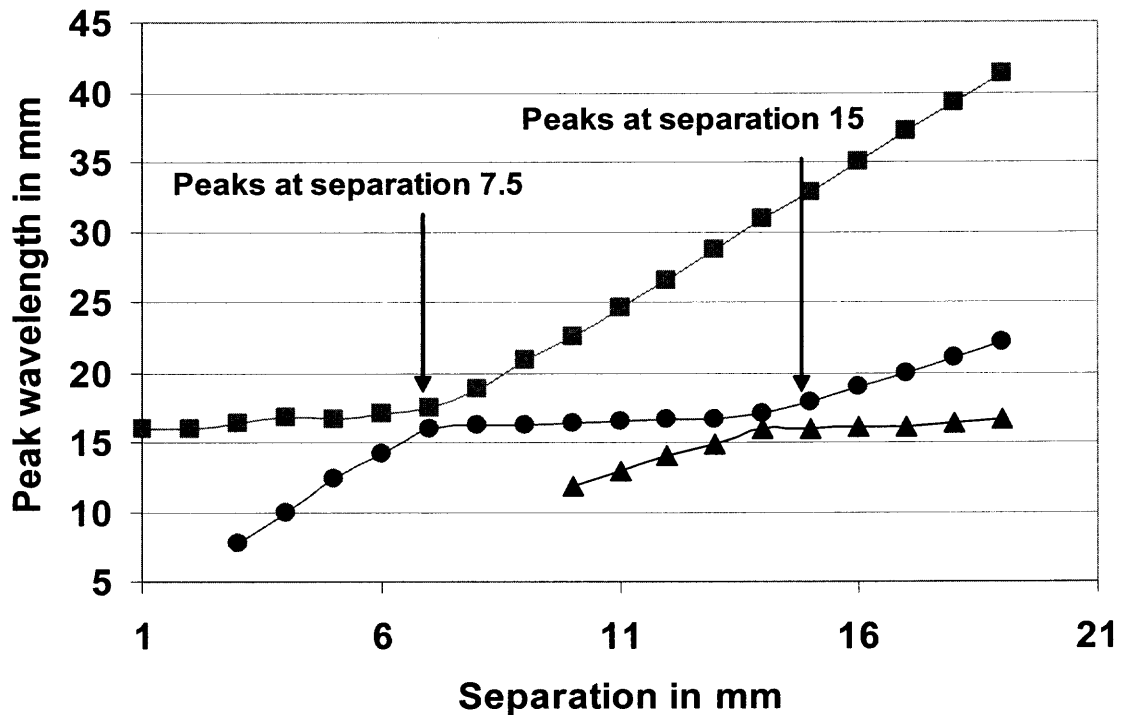


Figure 3.33 Resonance and stacking mode peaks for Simple Cubic crystal calculated with Transmission Line Theory.

Starting with a small separation of 4mm, the peak reflection wavelengths for resonance and stacking modes are plotted depending on the separation of layers. At 7.5 mm, the wavelengths of the resonance and fundamental stacking modes have about the

same value. These modes interact strongly, and according to the non-crossing rule of interacting oscillators, the stacking mode continues with values of the resonance mode, while the values of the resonance mode are replaced by the fundamental stacking mode. A similar situation appears at separation of 15 mm for resonance and the first order stacking modes. A peak appears at around 16 mm for all separations.

3.3.2 BCC Photonic Crystals

Figure 3.26(b) shows three layers of BCC PC. The first layer consists of four spheres with adjacent spheres apart by lattice distance 'a'. The second layer is similar to the first layer but shifted diagonally by $(\sqrt{2}*a)$ in both directions. Hence one sphere appears at the center. The periodicity constant remains the same as the crystal lattice. The separation 's' between the layers is 7.5 mm unlike Cubic PC where 's' is 15 mm.

3.3.2.1 Dependence on Number of Layers

3.3.2.1.1 Transmission for Crystal Lattice of 15 mm Reflection peaks are shown in Figure 4.8 for the BCC PC with numbers of layers varying from 1 to 10, and $a = 15$ mm, $d = 6.35$, and $s = 7.5$ mm,

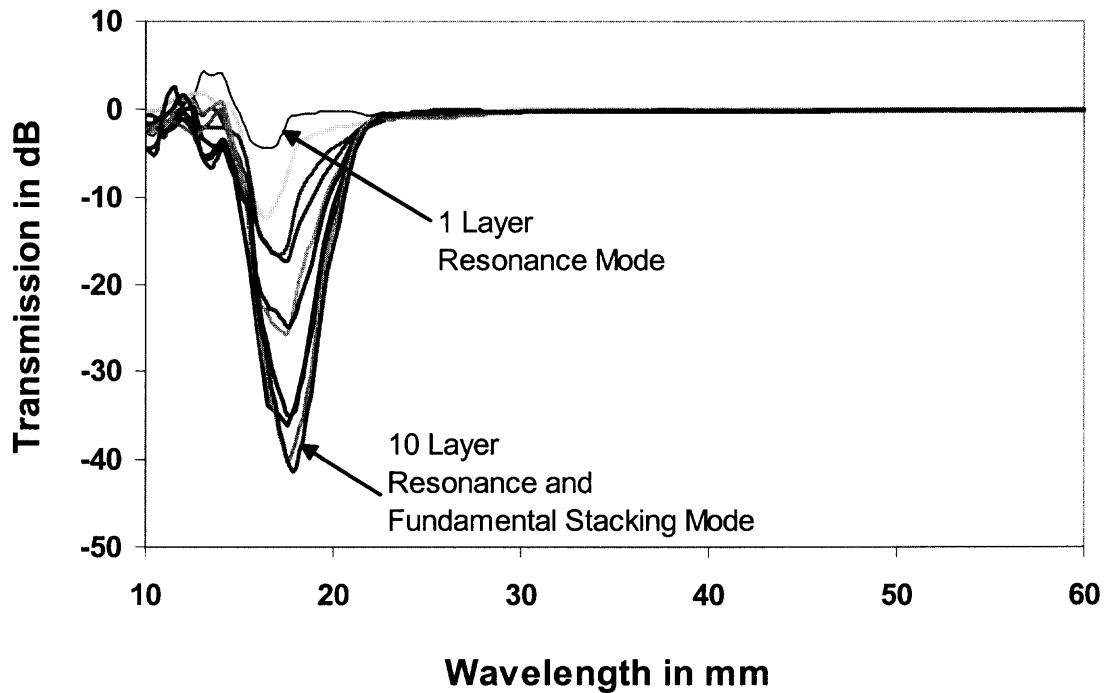


Figure 3.34 Micro-Stripes calculated transmission of a BCC crystal with 1 to 10 stacked layers. The parameters of the crystal are $a = 15$ mm, $d = 6.35$, $d_b = 6.35$ mm and $s = 7.5$ mm.

As seen in section 3.3.1, Cubic PC, the fundamental peak appears at approximately at $2 \cdot s$. Here for BCC PC $s = 7.5$ mm, so the fundamental stacking mode is expected to appear at 15 mm and the resonance mode also at 15 mm. And due to this interaction both the peaks appear at the broad-peak around 18 mm. The higher order stacking mode appears at shorter wavelength region.

3.3.2.1.2 Transmission for Crystal Lattice of 20 mm

For lattice distance of

20 mm, transmission was observed by J. Tobias experimentally¹⁷, shown in Figure 3.35, and compared with simulations. The number of layers is varied from 1 to 6. The other parameters are $d = 6.35$ mm, $a = 20$ mm and $s = 10$ mm.

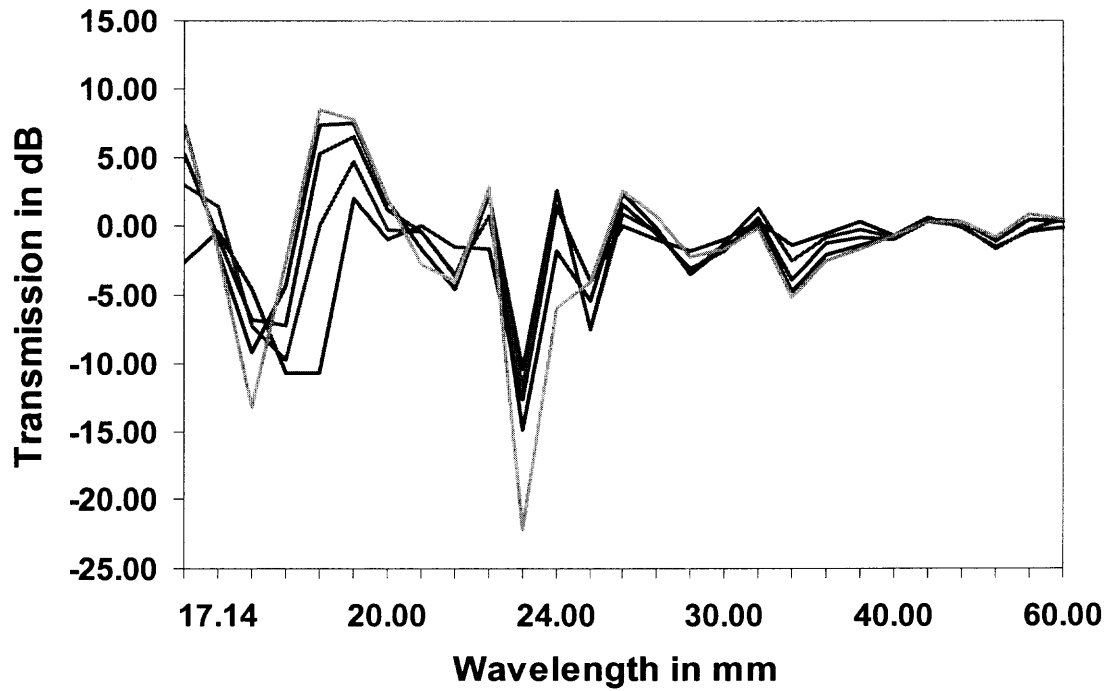


Figure 3.35 Experimentally measured transmission of BCC Crystal with $a = 20$ mm. The crystal parameters are $d = 6.35$ mm, $db = 6.35$ mm and $s = 10$ mm.

The experimental spectrum of Fig.3.35 shows two peaks, one at 18 mm and the other at 22 mm. the interpretation is done with the simulations shown in Fig.3.36.

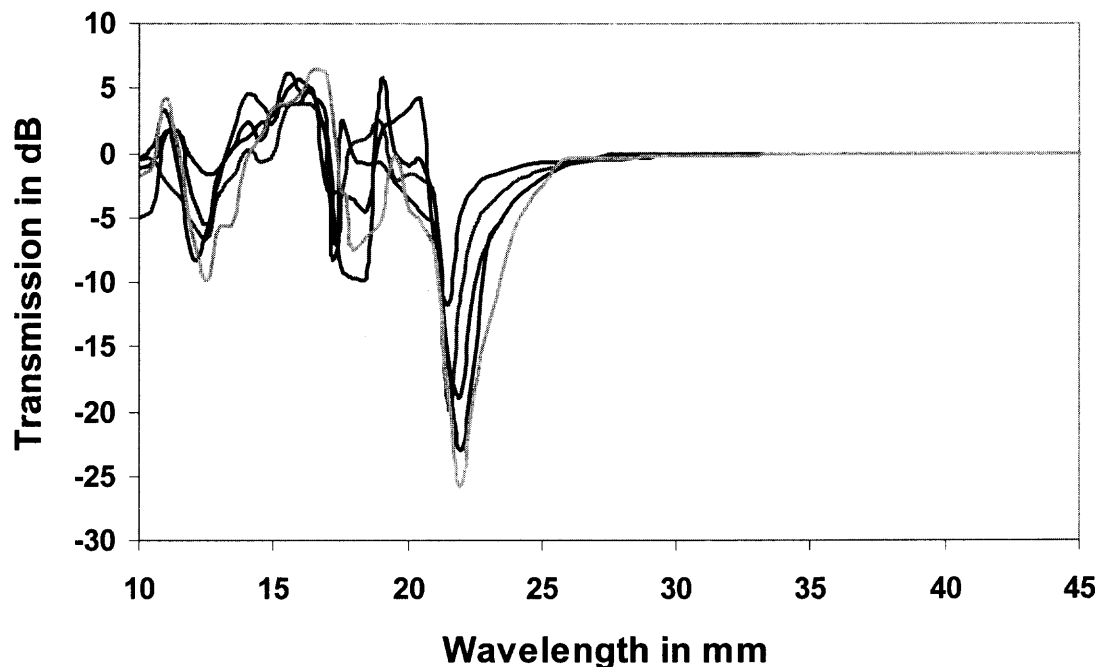


Figure 3.36 Micro-Stripes calculated transmission of a BCC crystal with 1 to 6 stacked layers. The parameters of the crystal are $a = 20$ mm, $d = 6.35$, $d_b = 6.35$ mm and $s = 10$ mm.

The resonance mode is expected at wavelength around 20 mm. The fundamental stacking mode appears at twice the separation of the layers and should have wavelength $2a/2$, that is also at 20 mm. Taking into account the consideration of Section 4.2.4., we assign the resonance mode to 18 mm and the fundamental stacking mode to 22 mm. The first order stacking mode is at 12 mm.

3.3.2.2 Transition of BCC to Simple Cubic Photonic Crystal for $a = 15$

In order to confirm the assignment of resonance, fundamental stacking and higher order stacking modes, the transition of BCC to Cubic PC was demonstrated by simulations. We refer to Figure 4.2 for the simple Cubic PC and Figure 4.8 for the BCC PC, both calculations are done for $a = 15$.

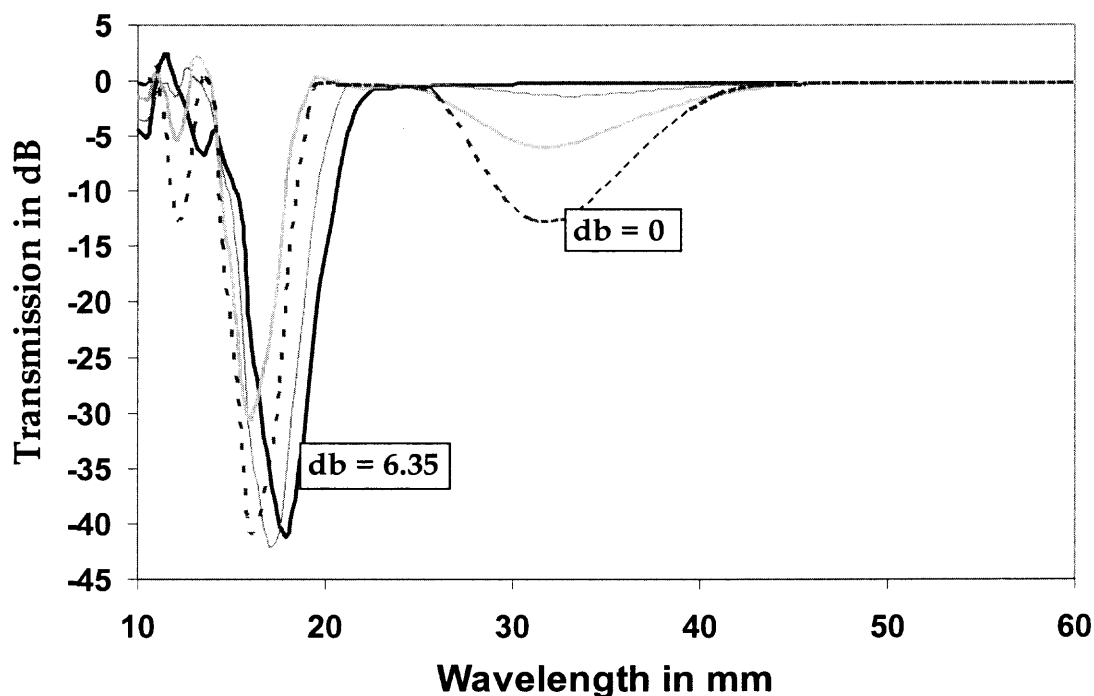


Figure 3.37 Transition from Simple Cubic to BCC by increasing center diameter 'db' in steps of 0, 4, 5 and 6.35mm.

With $d_b = 6.35$ mm, all the spheres have the same diameter and this represents a perfect BCC structure. The diameter of the center sphere d_b is reduced in steps of 6.35, 5, 4 to 0 mm. As d_b is reduced, the resonance mode shifts towards shorter wavelength and the fundamental stacking mode appears. Shifting of resonance mode to shorter wavelength shows less interaction between the resonance mode and fundamental stacking mode as in BCC and more interaction between resonance mode and first order stacking mode as in Simple Cubic PC. Also as d_b reduces, the higher order stacking mode begins to appear. The resonance mode shifts from 18 mm in BCC to 16 mm in Simple Cubic PC. The fundamental stacking mode appears at 32 mm and the higher order modes at 12 mm. This is in exact agreement with the simulations shown in Figure 3.37.

3.3.3 FCC Photonic Crystal

Figure 3.26(c) shows an FCC PC. Taking the smallest periodicity constant for the first layer, we have a cubic layer with periodicity constant of $(a/\sqrt{2})$. The second layer has the same periodicity constant but the spheres are displaced by $\frac{1}{2}$ of the periodicity constant. The separation between layers is 7.5 mm.

3.3.3.1 Experimental Result of Transmission through FCC PC

FCC PC has been investigated experimentally by Serpenguzel¹⁶, having $a = 15$ mm and $d = 6.35$ mm.

Figure 3.28 shows the normal incidence transmission through the crystal.

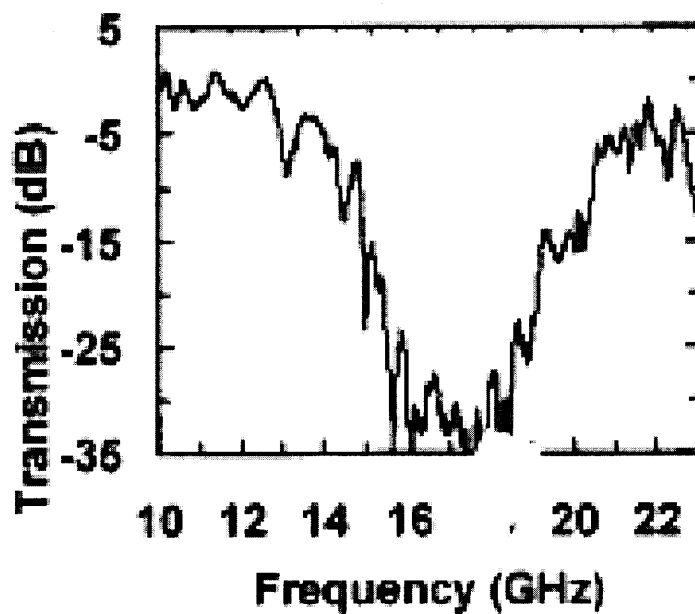


Figure 3.38 Experimental result for FCC PC by Serpenguzel with $a = 15$ mm and $d = 6.35$ mm.

A broad-peak is seen at a wavelength of around 17GHz i.e. 17.64mm.

3.3.3.2 Simulations of Transmission through FCC PC

Figure 3.39 shows the

simulated result using $a = 15\text{mm}$ and $d = 6.35\text{mm}$.

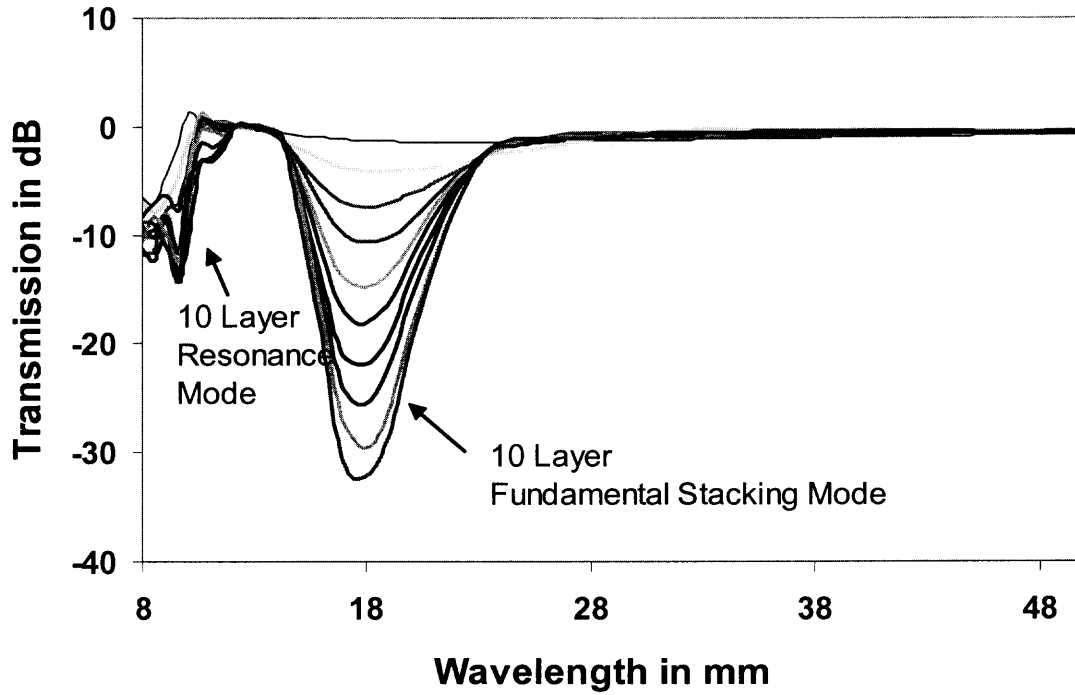


Figure 3.39 Micro-Stripes calculated transmission of an FCC crystal with 1 to 10 stacked layers. The crystal parameters are $a = 15\text{mm}$ and $d = 6.35\text{mm}$.

A broad peak is seen at 17.34mm in the simulation results which is more or less the same at the experimental result in Figure 3.39. The fundamental stacking mode is expected around twice the separation of the layers, $s = 7.5\text{mm}$, that is 15mm, and therefore we assign the resonance of the stacking mode to 18mm. The resonance mode was expected around the periodicity constant $(a/\sqrt{2})$, equal 10.6mm, appearing in the simulations at around 10mm. This resonance mode does not appear in the experimental results as it falls outside the wavelength range studied by Serpenguzel¹⁶.

3.3.4. Summary

The interpretation of the transmission spectra were done using the layered structure approach with resonance mode of one layer and stacking mode of a set of layers. For the simple Cubic crystal, the resonance mode has wavelength at around the lattice constant while the stacking mode has wavelength twice the lattice constant. As result, the first order stacking mode has a similar wavelength as the resonance mode, but there is little interaction because of the lined up layers, and the two peaks appear close together. The BCC crystal has layers separated at $\frac{1}{2}$ of the lattice constant, and every second, fourth and so on, layer is shifted. The fundamental stacking mode and the resonance mode have about the same wavelength, but the sifting of second, fourth and so on, layer and also the smaller distances between the spheres results in much stronger interaction, and resonance mode and fundamental stacking mode appear separated. The interpretation of the FCC crystals follows very much that of the BCC crystal.

CHAPTER 4

DISCUSSIONS

4.1 Single Layer Thick Metal Meshes

The simulations of the transmittance of single layer thick meshes of rectangular structure with cross, square and circular shaped openings results in a minimum at the Wood anomaly, and peaks for wave guide mode and resonance mode. The term “interaction” of two modes is used in the sense of perturbation theory, which is the wavelength of the resulting mode is the wavelength of the original mode, shifted by the interaction term.

The results of the cross shaped meshes is in excellent agreement with experimental data of samples produced with high quality. The wave guide mode appears at wavelength, equal to periodicity constant and due to its interaction with the resonance mode, the resonance mode shifts the peaks to longer wavelength for larger openings. The transmittance intensity of wave guide mode increases with increase in thickness of the mesh.

The simulations of the square shaped meshes agree well with the infrared spectra of commercially available meshes of periodicity constants in the range of 12 to 25 and normalized thickness 0.3 to 0.16. The resonance mode shifts with larger openings to longer wavelength and the wave guide mode appears close to wavelength, equal to periodicity constant and shows less interaction with the resonance modes as found for the cross shaped meshes.

The simulations of the circular shaped meshes is similar to the square shaped meshes, except that the resonance mode shifts less to longer wavelength. This may be

used for the design of a single narrow band filter, superior over cross and square shaped meshes filters having a band width of about 10% and high transmittance of 84%. The simulation shows also that the spectrum published by Ebbesen, Grupp and co-workers²⁸ in the near infrared is a peak of surface waves, generated by induction.

The simulations of the transmittance of thick single meshes of hexagonal structure with hexagonal shaped openings results in a minimum transmission at the Wood anomaly at a wavelength corresponding to the smaller of the reciprocal lattice vectors, and peaks for wave guide mode and resonance mode appear as one peak.

The simulations agree very well with experimental work in the far infrared, for resonance and wave guide mode. The shift of the resonance mode into the region of the waveguide modes has been observed also in the very short infrared region and indicates that the Drude model of the conductivity, as used in all simulations of gratings and meshes in the infrared, hold well for wavelength longer than the visible light. Experimental hexagonal structures have been produced in the sub millimeter wave region and interpreted with the mode wavelength of a single hole, $\lambda_R = 1.71d$. In comparison, the relation between resonance wavelength and diameter of the openings has been found to be $0.6g + 0.68d$ for a set of experimental results in the far infrared. There is agreement when the resonance wavelength is equal to the (larger) periodicity constant.

4.2 Photonic Double Layer of Thick Cross Shaped Inductive Meshes

The simulation of the photonic double layers shows the propagation of resonance and wave guide modes through a separation between equal meshes. For thin meshes without wave guide modes, the resonance mode changes intensity and wavelength depending on

the gap width. This can be used for the design of switches and modulators. For larger separations, the stacking modes are observed. For thicker meshes with wave guide modes, the resonance mode appears for all separations, the wave guide mode is changed, depending on the separation, as well as the appearance of the stacking mode. These double layers may be used as tunable filters.

4.3 Metallodielectric Photonic Crystals

The simulations of the photonic crystals of Simple Cubic and Body-centered Cubic crystals in the millimeter region agree very well with the experimental data. For the simple cubic crystal, the simulations of the resonance mode and the fundamental, first and second order stacking mode agree very well with the experimental data, except the second order was not in the range of measurements. The same was found for the body-centered cubic crystal, agreement the resonance mode, the fundamental and first order stacking mode, except the first order was not in the range of measurements. The separation of the resonance and fundamental stacking mode for the body-centered Cubic crystal, in comparison to the simple cubic crystal, was attributed to interaction of the shift to the aligned layer configuration.

The simulations of the face centered cubic crystal are in agreement with published work for the fundamental stacking mode, the resonance mode was out of the range of experimental observations.

CHAPTER 5

CONCLUSIONS

The Micro-Stripes program, used at normal incidence, simulates the transmittance of inductive and capacitive meshes in excellent agreement with experimental data and may be considered being equivalent to experiments. The Drude model approximation of the conductivity can be used as input data in the entire infrared region.

The interpretation of the transmittances of metal meshes may be done with the mode model, which is using the resonance mode for thin meshes, and in addition the wave guide mode for thick meshes. Filters of narrow band width and high peak transmittance may be designed with single layer thick metal meshes, choosing appropriate available geometrical parameters and high conductivity.

The transmittance of Photonic Double layers needs for the interpretation, in addition to resonance and wave guide mode, the stacking modes. Choice of the geometrical parameters and variation of the separations between the layers, can be used for the design of switches and tunable filters.

The transmittance of Photonic Crystals was interpreted with the layer-theory. A single layer was presented by a capacitive mesh and the resonance wavelength of one layer and the stacking modes of the equally spaced layers were used for the interpretation of all experimentally observed peaks in the simple cubic, body centered cubic and face centered cubic crystal lattice. The differences of interaction of aligned and non-aligned layers played a significant role in the interpretation of the transmittance of body centered and face centered cubic crystals.

REFERENCES

1. W. Culshaw, "High Resolution Millimeter wave Fabry Perot interferometer," IRE Trans. MTT-8, 182, 1960.
2. R. Ulrich, K.F. Renk, and L. Genzel, "Tunable submillimeter interferometers of the Fabry-Perot type," IEEE Trans. Micro-wave Theory Tech, MTT-11, 363-371, 1963.
3. R. Ulrich, "Far-infrared properties of metallic mesh and its complementary structures," Infrared Physics, 7, 37, 1967.
4. G.M. Ressler and K.D. Möller, "Far infrared bandpass filters and measurements on a reciprocal grid," Applied Optics, 6, 893-896, May 1967.
5. R. Ulrich, "Interference filters for the far infrared," Infrared Physics, 7, 1987- 1966, 1967.
6. S.T. Chase and R.D. Joseph, "Resonant array bandpass filters for the far infrared," Applied Optics, 22, 1775-1779, June 1983.
7. B.J. Munk, "Frequency selective surfaces," John Wiley & Sons, Inc., 2000.
8. L.B. Whitbourn and R.C. Compton, "Equivalent-circuit formulas for metal grid reflectors at a dielectric boundary," Applied Optics, 24, 217, January 1985.
9. M. Rebbert, P. Isaacson, Jacqueline Fischer, M. A. Greenhouse, J. Grossman, M. Peckerar, and H. A. Smith, "Microstructure technology for fabrication of metal mesh grids," Applied Optics 33, 1286, March 1994.
10. D. W. Porterfield, J. L. Hesler, R. Densing, E. R. Mueller, T.W. Crowe, and R.M. Weikle II, "Resonant metal-mesh bandpass filters for the far infrared," Applied Optics 33, 6046, September 1994.
11. K.D. Möller, J. Warren, J.B. Heaney, and C. Kotecki, "Cross-shaped bandpass filters for the near-and mid-infrared wavelength regions," Applied Optics, 35, 6210-6215, November 1996.
12. R. Ruprecht, W. Bacher, P. Bley, M. Harmening, and W.K. Schomburg, "Untersuchungen an mikrostrukturierten bandpass filtern für das ferne Infrarot," Kfk Nachr. Jahrg. 23, 2-91, 18-123, 1991.

13. J. S. McCalmont, M. M. Sigalas, G. Tuttle, K.-M. Ho and C. M. Soukolis, "A layer by-layer metallic photonic band-gap structure," Applied Physics Letters, **68**, 2759-2761, 6 May 1996.
14. J. G. Fleming, S. Y. Lin, I. El-Kady, R. Biswas and K. M. Ho, "All-Metallic three dimensional photonic crystals with a large infrared bandgap," Nature, **417**, 52-55, 2002.
15. Karl D. Möller, Oren Sternberg, Haim Grebel, and Kenneth P. Stewart, "Near-field effects in multilayer inductive metal meshes," Applied Optics, **41**, 1942-1948, 1 April 2002.
16. Ali Serpengüzel, "Transmission Characteristics of Metallo-dielectric Photonic Crystals and Resonators," IEEE Microwave and Wireless Components Letters, **12**, 134-136, April 2002.
17. John M. Tobias, "Experimental studies of wave propagation in three-dimensional photonic crystals," PhD Thesis, May 2002
18. J. Li, I. Zhou, C. t. Chan, and P. Sheng, "Photonic Band Gap from a Stack of Positive and Negative Index Materials," Physical Review Letters, **90**, 083901-1 to 04, 2003.
19. Micro-Stripes Program Ver 6.0[Computer Software], Southborough, Massachusetts: Flomerics, 2002.
20. L. Martin-Moreno, F.J Garcia-Vidal, H.J. Lezec. K. M. Pellerin, T. Thio, J. B. Pendry, and T. W. Ebbesen, "Theory of Extraordinary Optical Transmission through Subwavelength Hole Arrays," Physical Review Letters, **86**, 1114-1117, 2002.
21. K.D. Möller, O. Sternberg, H. Grebel , Philippe Lalanne, "Thick inductive cross shaped metal meshes," Applied Physics, **91**, 9461-9465, 15th June 2002.
22. R. Ulrich, "Proceedings of the Symposium of Optical and Acoustical MicroElectronics", Vol. XXIII, New York, NY, (Polytechnic, Brooklyn, NY, 1974).
23. K.D. Möller and W.G. Rothschild, "Far Infrared Spectroscopy," New York: John Wiley & Sons, 1971.
24. T. Timusk and P. L. Richards, "Near Millimeter wave band-pass filters," Applied Optics, **20**, 1355-1360, 1981.
25. K. D. Möller, "Optics, learning by computing", Springer-Verlag, New York, 2002.

26. Naval Research Laboratory, Remote Sensors Division, 4555 Overlook Ave SW. Washington DC 20375-5351, Experiments conducted: June 2003.
27. Buckbee Mears St. Paul, 278 East 7th Street, St.Paul, Minnesota 55101, www.buckbeemears.com, Date Accessed: 16th June 2003.
28. D. E. Grupp, H. J. Lezec, T. W. Ebbesen, K. M. Pellerin, and T. Thio, "Crucial role of metal surface in enhanced transmission through subwavelength apertures," Applied. Physics Letters. *77*, 1569-1571, 2000.
29. P. G. Huggard, M. Meyringer, A. Schilz, K. Goller and W. Prettl, "Far infrared bandpass filters from perforated metal screens," *Appl.Opt.*, **33**, 39-44, 1994.